Stochastic Environmental Research and Risk Assessment (2020) 34:1457–1471
https://doi.org/10.1007/s00477-020-01831-y

ORIGINAL PAPER

Global and local diagnostic analytics for a geostatistical model based on a new approach to quantile regression

Víctor Leiva[1] · Luis Sánchez[2] · Manuel Galea[3] · Helton Saulo[4]

Published online: 29 July 2020

Abstract
Data with spatial dependence are often modeled by geoestatistical tools. In spatial regression, the mean response is described using explanatory variables with georeferenced data. This modeling frequently considers Gaussianity assuming the response follows a symmetric distribution. However, when this assumption is not satisfied, it is useful to suppose distributions with the same asymmetric behavior of the data. This is the case of the Birnbaum–Saunders (BS) distribution, which has been considered in different areas and particularly in environmental sciences due to its theoretical arguments. We propose a geostatistical model based on a new approach to quantile regression considering the BS distribution. Global and local diagnostic analytics are derived for this model. The estimation of model parameters and its local influence are conducted by the maximum likelihood method. Global influence is based on the Cook distance and it is compared to local influence, in both cases to detect influential observations, whose detection and removal can modify the conclusions of a study. We illustrate the proposed methodology applying it to environmental data, which shows this situation changing the conclusions after removing potentially influential observations. A comparison with Gaussian spatial regression is conducted.

Keywords Diagnostic techniques · Environmental data · Maximum likelihood method · R software · Spatial models

1 Introduction

The Birnbaum–Saunders (BS) distribution constantly arises in the applied statistical literature. In the last decades, it has been shown to be versatile and efficient in several fields of science, being widely studied, due to its theoretical justification, its good properties and its close relation with the Gaussian or normal model. The BS distribution is unimodal, with asymmetry to the right and support defined on the positive real numbers, in addition to being indexed by two parameters that control its shape and scale. The BS distribution has its origins in physics and engineering, being it derived to model a fatigue phenomenon related to crack development in metallic objects; see Leiva (2019). Recently, Budsaba et al. (2020) suggested a physical model of this phenomenon which shows exactly how Birnbaum and Saunders (1969) derived their distribution to fit the model of a crack development. However, at the present, the BS distribution has gained increasing popularity in diverse areas including business (Leiva et al. 2014, 2016b; Saulo et al. 2019; Sánchez et al. 2020a), industry (Huerta et al. 2019; Leiva et al. 2019), and medicine (Lemonte et al. 2015; Leao et al. 2018a, b), among other areas. Nevertheless, outside the material fatigue phenomenon where the BS distribution was originated, the field where it has been widely applied is air pollution (Ferreira et al. 2012; Saulo et al. 2013; Marchant et al. 2018, 2019; Cavieres et al. 2020) and natural phenomena (Garcia-Papani et al. 2018a, b; Martinez et al. 2019; Carrasco et al. 2020), that is, in environmental sciences. The

✉ Víctor Leiva
victorleivasanchez@gmail.com
https://www.victor.leiva.cl

[1] School of Industrial Engineering, Pontificia Universidad Católica de Valparaíso, Valparaíso, Chile

[2] Department of Mathematics and Statistics, Universidad de La Frontera, Temuco, Chile

[3] Department of Statistics, Pontificia Universidad Católica de Chile, Santiago, Chile

[4] Department of Statistics, Universidade de Brasília, Brasília, Brazil

reason for this increasing applicability of the BS distribution in environmental sciences is because Leiva et al. (2015) proposed a chemical-physical model which shows how the derivation of Birnbaum and Saunders (1969) can be adapted to fit environmental data. These applications have been conducted by an interdisciplinary, international group of researchers. Note also that the study of methodological and theoretical issues of the BS distribution has received growing interest and a considerable amount of work is available; see Leiva and Saunders (2015), Leiva (2016), Aykroyd et al. (2018), Balakrishnan and Kundu (2019), Dasilva et al. (2020) and references therein, which summarize most of the works to the date.

Standard regression models describe the mean response given values of the explanatory variables. Nevertheless, if the response has an asymmetrical distribution, the mean is not a suitable centrality measure to summarize the data. Quantile regression was proposed by Koenker and Bassett (1978), extending the median regression to the ordinary quantiles by using the regression context. We propose to model the median or other quantiles of the BS distribution by regression. Considering a spatial component in the modeling may improve the accuracy of an estimator of the mean (or median); see Diggle and Ribeiro (2007). A first idea of spatial quantile regression was suggested by Kostov (2009). Trzpiot (2013) derived a spatial regression model using the quantile function; see McMillen (2013) for some variants of spatial quantile regressions. Garcia-Papani et al. (2017, 2018a, b) introduced BS spatial models for the mean, which need multivariate BS distributions; see, for example, Kundu (2015), Lemonte et al. (2015), Sánchez et al. (2015), Marchant et al. (2016a, b) and Garcia-Papani et al. (2017, 2018a, b). BS quantile regression was introduced by Sánchez et al. (2020a) and spatial BS quantile regression by Sánchez et al. (2020b), but to the best of our knowledge, global and local influence diagnostics for the spatial BS quantile regression do not have been formulated to the date.

Diagnostic analytics plays a relevant role in statistical modeling, which can be divided into global and local influence techniques. The Cook distance and residuals are well-known and often used as measures of global influence for detecting the model adequacy; see Krzanowski (1998) and Leiva et al. (2016a). However, the local influence technique is currently very popular, which allows us to evaluate the local effect of perturbations on the estimates of parameters and then to detect potentially influential cases in different models; see, for example, Diaz-Garcia et al. (2003), Santana et al. (2011), Garcia-Papani et al. (2017), Tapia et al. (2019a, b), and Liu et al. (2020). Detection and removal of potentially influential cases can modify the conclusions of a study.

This research has as objective to derive a geostatistical model based on Birnbaum–Saunders quantile regression and its global and local influence diagnostics. We use a new quantile parameterization to generate the model, which permits us to consider a similar framework to generalized linear models, providing wide flexibility. A comparison with Gaussian spatial regression is performed, but with other natural competing models, as gamma, lognormal or Weibull, it is not possible because such models based on our new parameterization are not available in the literature.

In Sect. 2, we present the original parameterization of the multivariate BS distribution and a new parameterization of it to model quantiles. Section 3 proposes the model and provides estimation of its parameters based on the maximum likelihood (ML) method. Then, in Sect. 4, we derive global influence measures based on the Cook distance for detecting influential potentially observations. Section 5 introduces the local influence technique for the new model including two schemes of perturbation. Next, we illustrate the proposed methodology in Sect. 6 considering an example related to environmental data. Some conclusions and future works are given in Sect. 7. All the numerical calculations were carried out with the aid of the R software; see R-Team (2018). Mathematical details of our results are provided in the Appendix.

2 The BS distribution and a new parameterization

2.1 The BS distribution

A random variable T given by the stochastic represention

$$T = T(Z;\alpha,\sigma) = \sigma\left(\alpha Z/2 + \sqrt{(\alpha Z/2)^2+1}\right)^2, \qquad (1)$$

where $Z \sim \mathrm{N}(0,1)$, follows a BS distribution of shape ($\alpha > 0$) and scale ($\sigma > 0$) parameters. We use the notation $T \sim \mathrm{BS}(\alpha,\sigma)$ to indicate it.

Let the random vector $\boldsymbol{V} = (V_1,\ldots,V_n)^\top \in \mathbb{R}^n$ follow an n-variate normal distribution, which we denote as $\boldsymbol{V} \sim \mathrm{N}_n(\boldsymbol{\mu},\boldsymbol{\Gamma})$, where $\boldsymbol{\mu} = (\mu_i) \in \mathbb{R}^n$ is a mean vector and $\boldsymbol{\Gamma} = (\rho_{jk}) \in \mathbb{R}^{n\times n}$ is a variance-covariance matrix, with $\mathrm{rank}(\boldsymbol{\Gamma}) = n$. If $\boldsymbol{\mu} = \boldsymbol{0}_{n\times 1}$, that is, the null vector with $\boldsymbol{0}_{n\times 1}$ being an $n \times 1$ vector of zeros, we use the notation ϕ_n and Φ_n for the n-variate normal density and distribution function, respectively. Then, $\boldsymbol{T} = (T_1,\ldots,T_n)^\top \in \mathbb{R}^n_+$ is an $n \times 1$ random vector with n-variate BS distribution of parameters $\boldsymbol{\alpha} = (\alpha_1,\ldots,\alpha_n)^\top \in \mathbb{R}^n_+$, $\boldsymbol{\sigma} = (\sigma_1,\ldots,\sigma_n)^\top \in \mathbb{R}^n_+$, and $\boldsymbol{\Gamma} \in \mathbb{R}^{n\times n}$, if $T_i = T(V_i;\alpha_i,\sigma_i)$, for $i = 1,\ldots,n$, where the T function, with V instead of Z, is given in (1) and $\boldsymbol{V} = (V_1,\ldots,V_n)^\top \in \mathbb{R}^n \sim \mathrm{N}_n(\boldsymbol{0}_{n\times 1},\boldsymbol{\Gamma})$. Note from (1) that

$Z \sim \mathrm{N}(0,1)$ and then $\boldsymbol{\Gamma} \in \mathbb{R}^{n\times n}$ has its diagonal elements equal to one. Hence, the variance-covariance matrix $\boldsymbol{\Gamma}$ is also the correlation matrix of $\boldsymbol{V}$, but not of $\boldsymbol{T}$, although for simplicity we denote the n-variate BS distribution as $\boldsymbol{T} \sim \mathrm{BS}_n(\boldsymbol{\alpha}, \boldsymbol{\sigma}, \boldsymbol{\Gamma})$. The variance-covariance matrix of $\boldsymbol{T}$ is expressed as

$$\mathrm{Var}(\boldsymbol{T}) = \frac{1}{16}\boldsymbol{\Omega} \odot (\boldsymbol{\Gamma} \odot \boldsymbol{\Gamma} \odot \boldsymbol{\Xi} + 4\boldsymbol{\Upsilon}), \tag{2}$$

where $\boldsymbol{\Omega} = (\omega_{ij})$, $\boldsymbol{\Xi} = (\xi_{ij})$ and $\boldsymbol{\Upsilon} = (\upsilon_{ij})$ have elements $\omega_{ij} = \alpha_i^2\alpha_j^2\sigma_i\sigma_j$, $\xi_{ij} = \alpha_i\alpha_j$ and $\upsilon_{ij} = I(\alpha_i, \alpha_j, \rho_{ij})$, respectively, for $i,j = 1,\ldots,n$, and $\odot$ is the Hadamard product; see details in Marchant et al. (2016a) and Sánchez et al. (2020b). Thus, the density and distribution function of $\boldsymbol{T}$ are, respectively, given by

$$f_{\boldsymbol{T}}(\boldsymbol{t};\boldsymbol{\alpha},\boldsymbol{\sigma},\boldsymbol{\Gamma}) = \phi_n(\boldsymbol{A};\boldsymbol{\Gamma})\, a(\boldsymbol{t};\boldsymbol{\alpha},\boldsymbol{\sigma}),$$
$$F_{\boldsymbol{T}}(\boldsymbol{t};\boldsymbol{\alpha},\boldsymbol{\sigma},\boldsymbol{\Gamma}) = \Phi_n(\boldsymbol{A};\boldsymbol{\Gamma}),\ \boldsymbol{t} = (t_1,\ldots,t_n) \in \mathbb{R}_+^n,$$

where $\boldsymbol{A} = \boldsymbol{A}(\boldsymbol{t};\boldsymbol{\alpha},\boldsymbol{\sigma}) = (A_1,\ldots,A_n)^\top$, with

$$A_j = (1/\alpha_j)(\sqrt{t_j/\sigma_j} - \sqrt{\sigma_j/t_j}),$$

and $a(\boldsymbol{t};\boldsymbol{\alpha},\boldsymbol{\sigma}) = \prod_{j=1}^n a(t_j;\alpha_j,\sigma_j)$, with

$$a(t_j;\alpha_j,\sigma_j) = (1/(2\alpha_j\sigma_j))(\sqrt{\sigma_j/t_j} + \sqrt{(\sigma_j/t_j)^3}).$$

2.2 A new quantile parameterization of the BS distribution

Let $\boldsymbol{T} = (T_1,\ldots,T_n) \sim \mathrm{BS}_n(\boldsymbol{\alpha},\boldsymbol{\sigma},\boldsymbol{\Gamma})$ and $q \in (0,1)$ be a fixed value. Then, we have a new parameterization of the n-variate BS distribution by the transformation expressed as $(\boldsymbol{\alpha},\boldsymbol{\sigma},\boldsymbol{\Gamma}) \mapsto (\boldsymbol{\alpha},\boldsymbol{Q},\boldsymbol{\Gamma})$, where Q_i and σ_i are related by

$$Q_i = \frac{\sigma_i}{4}\gamma_\alpha^2, \tag{3}$$

with $\gamma_\alpha = \alpha_i z_q + (\alpha_i^2 z_q^2 + 4)^{1/2}$, for the marginal distribution of T_i, Q_i being the q-th quantile of the $\mathrm{BS}(\alpha_i,\sigma_i)$ distribution (Sánchez et al. 2020a), for all $i = 1,\ldots,n$, and z_q being the q-th quantile of the standard normal distribution. This new parameterization of the n-variate BS distribution is denoted by $\boldsymbol{T} \sim \mathrm{BS}_n(\boldsymbol{\alpha},\boldsymbol{Q},\boldsymbol{\Gamma})$, with density and distribution function given, respectively, by

$$\begin{aligned} &f_{\boldsymbol{T}}(\boldsymbol{t};\boldsymbol{\alpha},\boldsymbol{Q},\boldsymbol{\Gamma}) = \phi_n(\tilde{\boldsymbol{A}};\boldsymbol{\Gamma})\,\tilde{a}(\boldsymbol{t};\boldsymbol{\alpha},\boldsymbol{Q}),\\ &F_{\boldsymbol{T}}(\boldsymbol{t};\boldsymbol{\alpha},\boldsymbol{Q},\boldsymbol{\Gamma}) = \Phi_n(\tilde{\boldsymbol{A}};\boldsymbol{\Gamma}),\quad \boldsymbol{t} = (t_1,\ldots,t_n) \in \mathbb{R}_+^n, \end{aligned} \tag{4}$$

where $\tilde{\boldsymbol{A}} = (\tilde{A_1},\ldots,\tilde{A_n})^\top$, with

$$\tilde{A_j} = \frac{1}{\alpha_j\gamma_{\alpha_j}}\sqrt{\frac{4Q_j}{t_j}}\left(\frac{t_j\gamma_{\alpha_j}^2}{4Q_j} - 1\right),$$

$$\tilde{a}(\boldsymbol{t};\boldsymbol{\alpha},\boldsymbol{Q}) = \prod_{j=1}^n \frac{1}{\alpha_j\gamma_{\alpha_j}\sqrt{4Q_jt_j}}\left(\frac{\gamma_{\alpha_j}^2}{2} + \frac{2Q_j}{t_j}\right),$$

and γ_{α_j} being defined in (3).

2.3 A shape analysis of the BS distribution parameterized by its quantiles

From Fig. 1, note that some shapes of the density expressed in (4) and their corresponding level curves are shown, for $n = 2$, varying the parameters α (a)–(c) and Q (d)–(f).

3 Formulation and estimation of the geostatistical model

3.1 The BS spatial quantile regression model

To describe data dependent spatially, assume the stochastic process $\boldsymbol{T} = \{T(\boldsymbol{s}); \boldsymbol{s} \in \boldsymbol{D}\}$ defined on $\boldsymbol{D} \in \mathbb{R}^2$. We consider that $\boldsymbol{T}$ is stationary and isotropic, and that for spatial locations in $\boldsymbol{s}_i$, with $i = 1,\ldots,n$, the quantile function of the process may be formulated as

$$Q(T(\boldsymbol{s}_i)) = Q_i(\boldsymbol{\beta}) = h^{-1}(\boldsymbol{x}_i^\top\boldsymbol{\beta}),\quad i = 1,\ldots,n, \tag{5}$$

with h being a strictly monotone function of positive support and at least twice differentiable. Observe that $\boldsymbol{x}_i^\top = (1, x_{i2},\ldots,x_{ip})$ are the values of $p-1$ explanatory variables, with $x_{ij} = x_j(\boldsymbol{s}_i)$, for $j = 1,\ldots,p-1$, that is, x_{ij} is the value of the explanatory variable X_j at $\boldsymbol{s}_i$. Here, $\boldsymbol{\beta} = (\beta_0,\beta_1,\ldots,\beta_q)^\top$, for $q = p-1 < n$, corresponds to a vector of regression coefficients to be estimated. In addition,

$$(T(\boldsymbol{s}_1),\ldots,T(\boldsymbol{s}_n)) \sim \mathrm{BS}_n(\alpha\boldsymbol{I}_{n\times 1}, \boldsymbol{Q}(\boldsymbol{\beta}), \boldsymbol{\Gamma}),\ \alpha > 0, \tag{6}$$

Notice where α is a scalar shape parameter, $\boldsymbol{I}_{n\times 1}$ is an $n\times 1$ vector of ones, $\boldsymbol{\Gamma}$ is the $n\times n$ matrix defined in (4), and $\boldsymbol{Q}(\boldsymbol{\beta})^\top = (Q_1(\boldsymbol{\beta}),\ldots,Q_n(\boldsymbol{\beta}))$, with $Q_i(\boldsymbol{\beta})$ given in (5), for $i = 1,\ldots,n$. From (2), note that the variance-covariance matrix of the BS spatial quantile regression model can be written as

$$\mathrm{Var}(\boldsymbol{T}) = \frac{4\alpha^2}{\gamma_\alpha^4}(\boldsymbol{Q}(\boldsymbol{\beta})\boldsymbol{Q}(\boldsymbol{\beta})^\top) \odot (\alpha^2\boldsymbol{\Gamma} \odot \boldsymbol{\Gamma} + 4\,\boldsymbol{\Upsilon}). \tag{7}$$

Notice that the variance-covariance matrix of the BS spatial process stated in (7) depends on its quantile function.

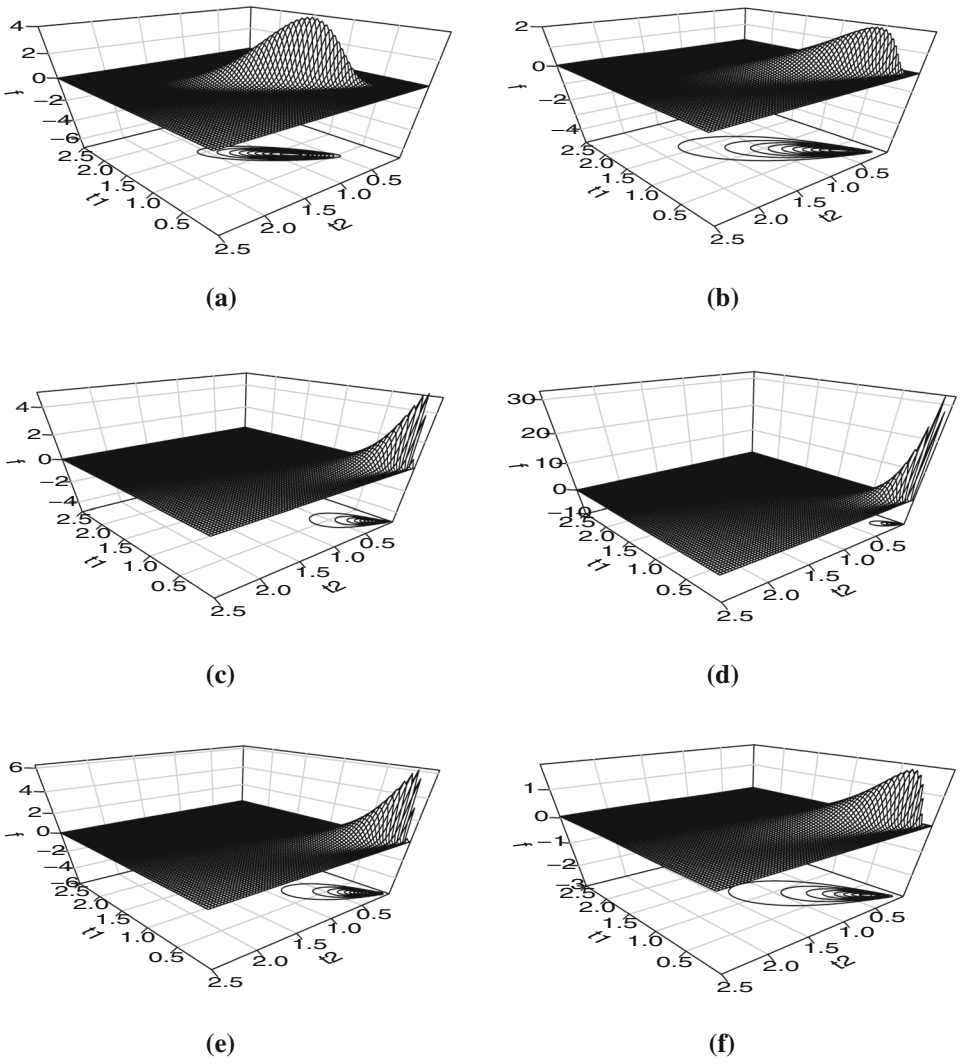

Fig. 1 Bivariate BS density plots for (**a**) $\alpha_i = 0.3$, (**b**) $\alpha_i = 0.7$, (**c**) $\alpha_i = 1.3$, with $Q_i = 1.0$, and (**d**) $Q_i = 0.3$, (**e**) $Q_i = 0.7$, (**f**) $Q_i = 1.3$, with $\alpha_i = 1.0$, for $i = 1, 2$ and $\rho = 0.9$

3.2 Modeling spatial dependence

Suppose that the spatial dependence is established by means of the $n \times n$ spatial correlation matrix $\boldsymbol{\Gamma}$, which is symmetric, non-singular and positive definite. The structure of this matrix is described by the Matérn model (Diggle and Ribeiro 2007) following an alternative parameterization proposed by Stein (1999). Thus, the elements of the matrix $\boldsymbol{\Gamma}$ are given by

$$\rho_{ij} = \begin{cases} 1, & i = j, \\ \dfrac{\varphi^{\delta}}{2^{\delta-1}\Gamma(\delta)} h_{ij}^{\delta} K_{\delta}(h_{ij}\,\varphi), & i \neq j, \end{cases} \tag{8}$$

where $\delta > 0$ is a shape parameter; Γ is the usual gamma function; h_{ij} is the Euclidean distance between the locations $\boldsymbol{s}_i$ and $\boldsymbol{s}_j$, that is, $h_{ij} = ||\boldsymbol{s}_i - \boldsymbol{s}_j||$; $\varphi > 0$ is a parameter known as the inverse spatial dependence radius (Zhang and Wang 2010) and also related to a parameter named microergodic by Stein (1999); and K_{δ} is the modified Bessel function of the third kind of order δ; see Gradshteyn and Ryzhik (2000). Note that the expression defined in (8) can be written in matrix form as

$$\boldsymbol{\Gamma} = \boldsymbol{\Gamma}(\varphi) = \boldsymbol{I}_n + \frac{\varphi^{\delta}}{2^{\delta-1}\Gamma(\delta)} \boldsymbol{J} \odot \boldsymbol{H}_{\delta} \odot \boldsymbol{K}_{\delta}, \tag{9}$$

where $\boldsymbol{I}_n$ is the $n \times 1$ identity matrix; $\boldsymbol{J}$ is a matrix with diagonal elements equal to zero and all other elements are ones; $\boldsymbol{H}_{\delta} = (h_{ij}^{\delta})$ and $\boldsymbol{K}_{\delta} = (K_{\delta}(\varphi\, h_{ij}))$. Table 1 provides some special members of the Matérn family.

Table 1 Special members of the Matérn correlation function

Shape parameter	Spatial correlation	Model
$\delta = 1/2$	$r(h) = \exp(-h\,\varphi)$	Exponential
$\delta = 1$	$r(h) = h\,\varphi\,K_{\delta}(h\,\varphi)$	Whittle
$\delta \to \infty$	$r(h) = \exp(-(h\,\varphi)^2)$	Gaussian

3.3 Estimation of model parameters

For the spatial model formulated in (5), as usual, we consider the shape parameter δ of the Matérn model to be a fixed value. Thus, the $(p+2)\times 1$ parameter vector of the BS spatial quantile regression model to be estimated is $\boldsymbol{\theta}=(\boldsymbol{\beta}^\top,\varphi,\alpha)^\top$, where $\boldsymbol{\beta}$ are the regression coefficients, φ is the spatial correlation parameter, and α is the shape parameter of the BS distribution, which is assumed to be constant but unknown in the BS spatial process. Therefore, by using the observations $\boldsymbol{t}=(t_1,\ldots,t_n)$, the corresponding BS spatial quantile regression parameter can be estimated by the ML method with log-likelihood function for $\boldsymbol{\theta}$ defined as

$$\ell(\boldsymbol{\theta})=-\frac{n}{2}\log(2\pi)-\frac{1}{2}\log(|\boldsymbol{\Gamma}|)-\frac{1}{2}\tilde{\boldsymbol{A}}^\top\boldsymbol{\Gamma}^{-1}\tilde{\boldsymbol{A}}+\log(\tilde{a}), \tag{10}$$

where $\tilde{\boldsymbol{A}}=\tilde{\boldsymbol{A}}(\boldsymbol{t};\alpha\boldsymbol{1}_{n\times 1},\boldsymbol{Q})$ and $\tilde{a}=\tilde{a}(\boldsymbol{t};\alpha\boldsymbol{1}_{n\times 1},\boldsymbol{Q})$, with $\boldsymbol{Q}=\boldsymbol{Q}(\boldsymbol{\beta})$ given from (6), and $\boldsymbol{\Gamma}=\boldsymbol{\Gamma}(\varphi)$ given in (9). By taking the derivative of (10), with respect to $\boldsymbol{\theta}$, allows us to obtain the $(p+2)\times 1$ score vector given by

$$\begin{aligned}\dot{\ell}(\boldsymbol{\theta})&=\left(\left(\frac{\partial\ell(\boldsymbol{\theta})}{\partial\boldsymbol{\beta}}\right)^\top,\frac{\partial\ell(\boldsymbol{\theta})}{\partial\varphi},\left(\frac{\partial\ell(\boldsymbol{\theta})}{\partial\alpha}\right)^\top\right)^\top\\&=\left(\dot{\ell}_{\beta_1},\ldots,\dot{\ell}_{\beta_p},\dot{\ell}_\varphi,\dot{\ell}_\alpha\right)^\top,\end{aligned}$$

where

$$\begin{aligned}\dot{\ell}_{\beta_j}&=-\tilde{\boldsymbol{A}}^\top\boldsymbol{\Gamma}^{-1}\frac{\partial\tilde{\boldsymbol{A}}}{\partial\beta_j}+\frac{\partial}{\partial\beta_j}(\log(\tilde{a})),\\\dot{\ell}_\varphi&=-\frac{1}{2}\operatorname{tr}\left(\boldsymbol{\Gamma}^{-1}\frac{\partial\boldsymbol{\Gamma}}{\partial\varphi}\right)+\frac{1}{2}\tilde{\boldsymbol{A}}^\top\boldsymbol{\Gamma}^{-1}\frac{\partial\boldsymbol{\Gamma}}{\partial\varphi}\boldsymbol{\Gamma}^{-1}\tilde{\boldsymbol{A}},\\\dot{\ell}_\alpha&=-\tilde{\boldsymbol{A}}^\top\boldsymbol{\Gamma}^{-1}\frac{\partial\tilde{\boldsymbol{A}}}{\partial\alpha}+\frac{\partial}{\partial\alpha}(\log(\tilde{a})),\end{aligned}$$

with $\partial\tilde{\boldsymbol{A}}/\partial\beta_j=(\partial\tilde{A}_k/\partial\beta_j)$ and $\partial\tilde{\boldsymbol{A}}/\partial\alpha=(\partial\tilde{A}_k/\partial\alpha)$, whose elements are expressed as

$$\begin{aligned}\frac{\partial\tilde{A}_k}{\partial\beta_j}&=-\frac{1}{\alpha\gamma_\alpha\sqrt{t_kQ_k}}\left(\frac{t_k\gamma_\alpha^2}{4Q_k}+1\right)\frac{1}{h'(Q_k)}x_{kj},\\\frac{\partial\tilde{A}_k}{\partial\alpha}&=\sqrt{\frac{4Q_k}{t_k}}\left(-\frac{1}{(\alpha\gamma_\alpha)^2}(\gamma_\alpha+\alpha\gamma'_\alpha)\left(\frac{t_k\gamma_\alpha^2}{4Q_k}-1\right)+\frac{\gamma'_\alpha t_k}{2\alpha Q_k}\right),\\\frac{\partial}{\partial\beta_j}(\log(\tilde{a}))&=\sum_{k=1}^{n}\left(-\frac{1}{2Q_k}+\frac{4}{t_k\gamma_\alpha^2+4Q_k}\right)\frac{1}{h'(Q_k)}x_{kj},\\\frac{\partial}{\partial\alpha}(\log(\tilde{a}))&=-\frac{n}{\alpha\gamma_\alpha}(\gamma_\alpha+\alpha\gamma'_\alpha)+\sum_{k=1}^{n}\frac{2t_k\gamma_\alpha\gamma'_\alpha}{t_k\gamma_\alpha^2+4Q_k}.\end{aligned}$$

In addition, $\partial\boldsymbol{\Gamma}/\partial\varphi=(\partial\rho_{ij}/\partial\varphi)$, with elements defined as

$$\frac{\partial\rho_{ij}}{\partial\varphi}=\begin{cases}\dfrac{h_{ij}^\delta}{2^{\delta-1}\Gamma(\delta)}\left(\delta\varphi^{\delta-1}K_\delta(\varphi\,h_{ij})+\varphi^\delta K'_\delta(\varphi\,h_{ij})h_{ij}\right), & i\neq j;\\ 0, & i=j;\end{cases}$$

where $K'_\delta(u)=\mathrm{d}K_\delta(u)/\mathrm{d}u$. To estimate $\boldsymbol{\theta}$, $\dot{\ell}(\boldsymbol{\theta})=\boldsymbol{0}_{(p+2)\times 1}$ must be solved. Note that this system does not have an analytical solution. Then, $\widehat{\boldsymbol{\theta}}$ must be obtained with iterative procedures for non-linear systems; see Nocedal and Wright (1999) and Lange (2001).

4 Global influence diagnostics

4.1 Likelihood distance

A global influence technique of case-deletion is based on the likelihood distance (LD) and established as

$$\mathrm{LD}_i(\boldsymbol{\theta})=2(\ell(\widehat{\boldsymbol{\theta}})-\ell(\widehat{\boldsymbol{\theta}}_{(i)})),\quad i=1,\ldots,n, \tag{11}$$

where ℓ is the log-likelihood function, and $\widehat{\boldsymbol{\theta}},\widehat{\boldsymbol{\theta}}_{(i)}$ are, respectively, the ML estimates of $\boldsymbol{\theta}$ considering the full data set and the data set without case i; see Cook et al. (1988). The expression given in (11) measures the change in the LD with estimated parameters when case i is deleted and may be employed as global influence technique to assess the potential influence of this case.

4.2 Cook distance

The Cook distance (CD) is other global influence technique based on case deletion and an alternative to the measure defined in (11). This has been generalized to several non-normal models; see Desousa et al. (2018). The usual expression for the CD is given by

$$\mathrm{CD}_i(\boldsymbol{\theta})=(\widehat{\boldsymbol{\theta}}-\widehat{\boldsymbol{\theta}}_{(i)})^\top\boldsymbol{M}(\widehat{\boldsymbol{\theta}}-\widehat{\boldsymbol{\theta}}_{(i)}),\quad i=1,\ldots,n, \tag{12}$$

where $\boldsymbol{M}$ is an appropriately chosen positive definite matrix, which can be, for example, the inverse of the asymptotic covariance matrix. Thus, a measure based on the CD established in (12) is stated as

$$\mathrm{CD}_i^{(1)}(\boldsymbol{\theta})=(\widehat{\boldsymbol{\theta}}-\widehat{\boldsymbol{\theta}}_{(i)})^\top(-\ddot{\ell}_{(i)}(\widehat{\boldsymbol{\theta}}))(\widehat{\boldsymbol{\theta}}-\widehat{\boldsymbol{\theta}}_{(i)}),\quad i=1,\ldots,n, \tag{13}$$

where

$$\ddot{\ell}_{(i)}(\boldsymbol{\theta})=\frac{\partial\ell_{(i)}^2(\boldsymbol{\theta})}{\partial\boldsymbol{\theta}\partial\boldsymbol{\theta}^\top},$$

with $\ell_{(i)}$ being the log-likelihood function obtained after deleting case i. Note that

$$\boldsymbol{M}=(-\ddot{\ell}_{(i)}(\widehat{\boldsymbol{\theta}}))$$

defined in (12) is the inverse of $(-\ddot{\ell}_{(i)}(\widehat{\boldsymbol{\theta}}))^{-1}$, which is an estimate of the corresponding asymptotic covariance matrix. If n is too large, the computation of $\ddot{\ell}_{(i)}(\widehat{\boldsymbol{\theta}})$ may became hard and, in this case, $\ddot{\ell}(\widehat{\boldsymbol{\theta}})$ can be used instead of $\ddot{\ell}_{(i)}(\widehat{\boldsymbol{\theta}})$; see De Bastiani et al. (2018). Then, an alternative measure of global influence based on the CD expressed in (13) is given by

$$\mathrm{CD}_i^{(2)}(\boldsymbol{\theta}) = (\widehat{\boldsymbol{\theta}} - \widehat{\boldsymbol{\theta}}_{(i)})^\top(-\ddot{\ell}(\widehat{\boldsymbol{\theta}}))(\widehat{\boldsymbol{\theta}} - \widehat{\boldsymbol{\theta}}_{(i)}), \quad i = 1, \ldots, n. \tag{14}$$

4.3 Generalized Cook distance

Other measure based on the CD defined in (14) uses the first order approximation $\widehat{\boldsymbol{\theta}} - \widehat{\boldsymbol{\theta}}_{(i)} \approx \ddot{\ell}_{(i)}^{-1}(\widehat{\boldsymbol{\theta}})\dot{\ell}_{(i)}(\widehat{\boldsymbol{\theta}})$, which considers a Taylor expansion around $\widehat{\boldsymbol{\theta}}$, until the second order term, and the one-step-late Newton-Raphson estimate. This third measure based on (14) is expressed as

$$\mathrm{CD}_i^{(3)}(\boldsymbol{\theta}) = \big(\dot{\ell}_{(i)}(\widehat{\boldsymbol{\theta}})\big)^\top\big(\ddot{\ell}_{(i)}(\widehat{\boldsymbol{\theta}})\big)^{-1}\big(\dot{\ell}_{(i)}(\widehat{\boldsymbol{\theta}})\big), \; i = 1, \ldots, n, \tag{15}$$

where

$$\dot{\ell}_{(i)}(\widehat{\boldsymbol{\theta}}) = \frac{\partial \ell_{(i)}(\boldsymbol{\theta})}{\partial \boldsymbol{\theta}}.$$

Other alternative measures based on the CD similar to (15) can be seen in Garcia-Papani et al. (2018b). In many cases, $\mathrm{CD}_i(\boldsymbol{\theta})$ is preferred to $\mathrm{LD}(\widehat{\boldsymbol{\theta}}_{(i)})$, because of its heavier computational burden. A large value of $\mathrm{CD}_{(i)}(\boldsymbol{\theta})$ means that case i is potentially influential. A definition of what is large has been an unresolved aspect, but Cook et al. (1982) established this depends on each problem upon study.

5 Local influence diagnostics

5.1 Local influence distance based on normal curvature

The local influence technique examines the effect of small perturbations in the data and/or the model assumptions on the estimated parameters. Cook (1987) evaluated local influence considering

$$\mathrm{LD}(\boldsymbol{\theta}_{\boldsymbol{\omega}}) = 2(\ell(\widehat{\boldsymbol{\theta}}) - \ell(\widehat{\boldsymbol{\theta}}_{\boldsymbol{\omega}})), \tag{16}$$

with $\widehat{\boldsymbol{\theta}}$ and $\widehat{\boldsymbol{\theta}}_{\boldsymbol{\omega}}$ being the ML estimates of $\boldsymbol{\theta}$ in the proposed model and the model perturbed by $\boldsymbol{\omega}$, respectively. Cook (1987) analyzed the normal curvature of the influence graph $\mathrm{LD}(\boldsymbol{\theta}_{\boldsymbol{\omega}})$ around the non-perturbation point $\boldsymbol{\omega}_0$ in the direction of a unit vector $\boldsymbol{d}$. Cook (1987) showed that this curvature based on (16) takes the form

$$C_{\boldsymbol{d}} = 2|\boldsymbol{d}^\top \boldsymbol{B}\boldsymbol{d}|,$$

where

$$\boldsymbol{B} = -\boldsymbol{\Delta}^\top \ddot{\ell}(\widehat{\boldsymbol{\theta}})^{-1}\boldsymbol{\Delta}, \tag{17}$$

with $\ddot{\ell}(\widehat{\boldsymbol{\theta}})$ being the Hessian matrix, evaluated at $\boldsymbol{\theta} = \widehat{\boldsymbol{\theta}}$, and

$$\boldsymbol{\Delta} = \frac{\partial^2 \ell(\boldsymbol{\theta}; \boldsymbol{\omega})}{\partial \boldsymbol{\theta} \partial \boldsymbol{\omega}^\top} \tag{18}$$

being the perturbation matrix, evaluated at $\boldsymbol{\theta} = \widehat{\boldsymbol{\theta}}$ and $\boldsymbol{w} = \boldsymbol{w}_0$. Specific details of the perturbation matrix defined in (18) are shown in the Appendix. Because the maximum normal curvature $C_{\boldsymbol{d}max}$ is reached at $\boldsymbol{d}_{\max}$, which is the eigenvector associated with the largest absolute eigenvalue of the matrix $\boldsymbol{B}$, Cook (1987) stated that $\boldsymbol{d} = \boldsymbol{d}_{\max}$ is an important direction to pay attention. Thus, the plot of the i-th element (in absolute value) of $\boldsymbol{d}_{\max}$ versus the index i can detect observations that are (in a local manner) potentially influential on $\widehat{\boldsymbol{\theta}}$. The direction $\boldsymbol{d} = \boldsymbol{e}_i$, with $\boldsymbol{e}_i$ being a basis vector of $\mathbb{R}^n$ whose i-th coordinate is one and the others are zero, corresponds to other relevant direction to analyze. For such a direction, the normal curvature is given by

$$C_i = 2|b_{ii}|, \quad i = 1, \ldots, n,$$

where b_{ii} is the i-th element on the diagonal of the matrix $\boldsymbol{B}$ indicated in (17). When considering case i, if

$$C_i > 2\sum_{i=1}^{n}\frac{C_i}{n} = 2\bar{C}, \quad i = 1, \ldots, n,$$

then this case is potentially influential; see Lesaffre and Verbeke (1998).

5.2 Local influence distance based on conformal curvature

In addition to the normal curvature of Cook (1987), other measures of local influence have been studied and employed. Poon and Poon (1999) defined the conformal curvature as

$$B_i = \frac{C_i}{\mathrm{trace}(\boldsymbol{B})}, \quad i = 1, \ldots, n, \tag{19}$$

which demands a similar computational burden to C_i. The measure indicated in (19) is standard because it is invariant under conformal reparameterizations. Hence, it is not difficult to establish a cut-off point for it. According to Poon and Poon (1999), if for case i we obtain

$$B_i > 2\sum_{i=1}^{n}\frac{B_i}{n} = 2\bar{B}, \quad i = 1, \ldots, n,$$

where $\bar{B}$ is the arithmetic mean of the basic conformal curvatures, that is, of $B_1, \ldots, B_n$, then case i is potentially influential. Another cut-off point implies to consider case i as potentially influential if

$$B_i > \bar{B} + 2\mathrm{SD}(B), \quad i = 1, \ldots, n,$$

where $\mathrm{SD}(B)$ is the standard deviation (SD) of $B_1, \ldots, B_n$.

5.3 Perturbation scheme in the response

We assume the perturbation

$$\boldsymbol{T}_{\boldsymbol{\omega}}(\boldsymbol{s}) = \boldsymbol{T}(\boldsymbol{s}) + \boldsymbol{A}\boldsymbol{\omega},$$

where $\boldsymbol{A}$ is a symmetric, non-singular matrix and $\boldsymbol{\omega} = (\omega_1, \ldots, \omega_n) \in \mathbb{R}^n$ is a perturbation vector. It is clear that $\boldsymbol{\omega}_0 = \mathbf{0}_{n\times 1}$ is the non-perturbation vector. In this scheme, the perturbed log-likelihood function is given by

$$\ell(\boldsymbol{\theta}; \boldsymbol{\omega}) = -\frac{n}{2}\log(2\pi) - \frac{1}{2}\log(|\boldsymbol{\Gamma}|) - \frac{1}{2}\tilde{\boldsymbol{A}}_{\boldsymbol{\omega}}^{\top}\boldsymbol{\Gamma}^{-1}\tilde{\boldsymbol{A}}_{\boldsymbol{\omega}} + \log(\tilde{a}_{\boldsymbol{\omega}}), \tag{20}$$

where $\tilde{\boldsymbol{A}}_{\boldsymbol{\omega}} = (\tilde{A}_1(\boldsymbol{\omega}), \ldots, \tilde{A}_n(\boldsymbol{\omega}))^{\top}$ and $\tilde{a}_{\boldsymbol{\omega}} = \tilde{a}(\boldsymbol{t}(\boldsymbol{\omega}); \alpha, \boldsymbol{Q})$, with

$$\tilde{A}_k(\boldsymbol{\omega}) = A(t_k(\boldsymbol{\omega}); \alpha, Q_k), \quad k = 1, \ldots, n.$$

Zhu et al. (2007) established that the perturbation $\boldsymbol{\omega}$ is appropriate if and only if $\boldsymbol{G}(\boldsymbol{\theta}; \boldsymbol{\omega}_0) = c\boldsymbol{I}_n$, where $c > 0$ and

$$\boldsymbol{G}(\boldsymbol{\theta}; \boldsymbol{\omega}) = \mathrm{E}(\dot{\ell}(\boldsymbol{\theta}; \boldsymbol{\omega})\dot{\ell}^{\top}(\boldsymbol{\theta}; \boldsymbol{\omega})),$$

with $\dot{\ell}(\boldsymbol{\theta}; \boldsymbol{\omega}) = \partial\ell(\boldsymbol{\theta}; \boldsymbol{\omega})/\partial\boldsymbol{\omega}$. Obtaining the matrix $\boldsymbol{G}(\boldsymbol{\theta}; \boldsymbol{\omega}_0)$ can be a very difficult. In this paper, we assume that the form of $\boldsymbol{A}$ to obtain an appropriate perturbation $\boldsymbol{\omega}$ is the same obtained in Garcia-Papani et al. (2018b), that is,

$$\boldsymbol{A} = \left(\frac{\alpha}{4}\boldsymbol{\Gamma}^{1/2} - \frac{1}{\alpha}\boldsymbol{\Gamma}^{-1/2}\right)^{-1}, \tag{21}$$

where $\boldsymbol{\Gamma}^{1/2}$ is the square root matrix of $\boldsymbol{\Gamma}$, that is, $\boldsymbol{\Gamma}^{1/2}\boldsymbol{\Gamma}^{1/2} = \boldsymbol{\Gamma}$. For details of computations for this square root matrix, see De Bastiani et al. (2015). Therefore, we assume that an appropriate perturbation scheme for the response is given by

$$\boldsymbol{T}_{\boldsymbol{\omega}}(\boldsymbol{s}) = \boldsymbol{T}(\boldsymbol{s}) + \left(\frac{\alpha}{4}\boldsymbol{\Gamma}^{1/2} - \frac{1}{\alpha}\boldsymbol{\Gamma}^{-1/2}\right)^{-1}\boldsymbol{\omega}.$$

5.4 Perturbation in a continuous explanatory variable

Now, we perturb a continuous explanatory variable, labelled as X_l namely, and the other explanatory variables are not perturbed. Thus, we have

$$\boldsymbol{x}_{l,\boldsymbol{\omega}}(\boldsymbol{s}) = \boldsymbol{x}_l(\boldsymbol{s}) + \boldsymbol{A}\boldsymbol{\omega}, \quad \boldsymbol{x}_{j,\boldsymbol{\omega}}(\boldsymbol{s}) = \boldsymbol{x}_j(\boldsymbol{s}), \quad j \neq l, j = 1, \ldots, q,$$

where $\boldsymbol{\omega} \in \mathbb{R}^n$ and $\boldsymbol{\omega}_0 = \boldsymbol{\theta}_{n\times 1}$. Hence, in this scheme, the perturbed log-likelihood function is given by

$$\ell(\boldsymbol{\theta}; \boldsymbol{\omega}) = -\frac{n}{2}\log(2\pi) - \frac{1}{2}\log(|\boldsymbol{\Gamma}|) - \frac{1}{2}\tilde{\boldsymbol{A}}_{\boldsymbol{\omega}}^{\top}\boldsymbol{\Gamma}^{-1}\tilde{\boldsymbol{A}}_{\boldsymbol{\omega}} + \log(\tilde{a}_{\boldsymbol{\omega}}), \tag{22}$$

where $\tilde{\boldsymbol{A}}_{\boldsymbol{\omega}} = (\tilde{A}_1(\boldsymbol{\omega}), \ldots, \tilde{A}_n(\boldsymbol{\omega}))^{\top}$ and $\tilde{a}_{\boldsymbol{\omega}} = \tilde{a}(\boldsymbol{t}; \alpha, \boldsymbol{Q}(\boldsymbol{\omega}))$, with $\tilde{A}_k(\boldsymbol{\omega}) = A(t_k; \alpha, Q_k(\boldsymbol{\omega}))$, for $k = \overline{1, n}$. Once again, obtaining the matrix $\boldsymbol{A}$ for an appropriate perturbation in X_l can be a hard work. As in the case of the response perturbation with $\boldsymbol{A}$ given in (21), we assume that the most appropriate explanatory variable perturbation may be expressed as

$$\boldsymbol{x}_{t,\boldsymbol{\omega}}(\boldsymbol{s}) = \boldsymbol{x}_t(\boldsymbol{s}) + \left(\frac{\alpha}{4}\boldsymbol{\Gamma}^{1/2} - \frac{1}{\alpha}\boldsymbol{\Gamma}^{-1/2}\right)^{-1}\boldsymbol{\omega}.$$

5.5 Other perturbations

In order to illustrate the methodology of perturbation associated with the local influence technique, we consider only perturbations in the response and in a continuous explanatory variable. However, other schemes of perturbation of the local influence technique can also be considered for the BS spatial quantile regression model derived in this investigation. These perturbation schemes may be proposed to assess changes in the cases (that is, case-weight perturbation), in the scalar parameters α or φ, as well as in the correlation matrix $\boldsymbol{\Gamma}$. For instance, when perturbing the parameter α, we must consider

$$\alpha_i = \frac{\alpha}{\omega_i}, \quad i = 1, \ldots, n,$$

with $\omega_i > 0$; see Sánchez et al. (2020a). Similarly for perturbing the parameter φ. For perturbing the correlation matrix $\boldsymbol{\Gamma}$, see Marchant et al. (2016b).

6 Empirical illustrative example

6.1 The data set and exploratory analysis

The methodology presented in this paper is illustrated considering an environmental data set related to key nutrients in the soil. The data set belongs to $n = 82$ locations of an area in Brazil, where levels of magnesium (Mg) and calcium (Ca) are measured. Mg affects the development of the root system, while Ca is analyzed as a competitor of Mg for absorption of nutrients. The response variable (T) is the content of Mg in the soil (in cmolc/dm3)

and the explanatory variable (X) is the content of Ca in the soil (in cmolc/dm3).

Descriptive statistics for the vector of Mg values are summarized in Table 2. This summary shows the asymmetric behavior of the distribution of the response variable, which is also observed in the histogram of Fig. 2a, while the boxplot of the values of the response T allows us to observe two outliers, which are cases #12 and #47. A three-dimensional scatter plot of the response values is provided in Fig. 2b. The directional variogram of Fig. 2c indicates that there is no preferred direction, meaning an omni-directional semi-variogram is suitable. Hence, we can consider the associated stochastic process as isotropic.

6.2 Formulation, estimation of parameters, and comparison of models

We estimate the spatial dependence parameters assuming a variogram using the Matérn model with $\delta = 0.5$. Suppose that

$$(T(\boldsymbol{s}_1), \ldots, T(\boldsymbol{s}_n)) = (T_1, \ldots, T_n) \sim \mathrm{BS}_n(\alpha \boldsymbol{I}_{n\times 1}, \boldsymbol{Q}(\boldsymbol{\beta}), \boldsymbol{\Gamma}),$$

considering three cases for the link function h defined in (5), that is, logarithm, square root and identity functions, which are expressed, for $i = 1, \ldots, 82$, as

$$\begin{aligned} \log(Q(T(\boldsymbol{s}_i))) &= \boldsymbol{x}_i^\top \boldsymbol{\beta}, \\ \sqrt{Q(T(\boldsymbol{s}_i))} &= \boldsymbol{x}_i^\top \boldsymbol{\beta}, \\ Q(T(\boldsymbol{s}_i)) &= \boldsymbol{x}_i^\top \boldsymbol{\beta}, \end{aligned}$$

with $\boldsymbol{\beta} = (\beta_0, \beta_1)^\top$ being the regression coefficient vector and $\boldsymbol{x}_i^\top = (1, x_{i1})$ being the value of $\boldsymbol{X}_i$.

In order to compare spatial regression models, we employ the Schwarz Bayesian information criterion (BIC) and corrected Akaike information criterion (CAIC) stated as

$$\begin{aligned} \mathrm{BIC} &= d\log(n) - 2\ell(\widehat{\boldsymbol{\theta}}), \\ \mathrm{CAIC} &= 2d - 2\ell(\widehat{\boldsymbol{\theta}}) + \frac{2d^2 + 2d}{n - d - 1}, \end{aligned}$$

where $d = p + 2 = 4$ is the number of model parameters, $n = 82$ is the dimension of the data set, and $\ell(\widehat{\boldsymbol{\theta}})$ corresponds to the log-likelihood function for $\boldsymbol{\theta}$ of the underlying model evaluated at $\boldsymbol{\theta} = \widehat{\boldsymbol{\theta}}$. BIC and CAIC use the log-likelihood function and penalize a model with more parameters. When a small quantity of information is obtained from a model in relation a specific data set, then large values for BIC and CAIC are obtained for this model, which indicates that the model is less adequate than other with smaller BIC or CAIC. Then, the best model is that with the smallest value for the BIC or CAIC; see Ferreira et al. (2012). Table 3 reports the values of the log-likelihood function, CAIC and BIC for the model with link functions defined in (23). Also, we compare the models given in (23) with the Gaussian spatial regression model applied to the data set, which considers the description of the mean (or equivalently the median) with identity link function; see Table 3. Note that the BS model with square root link is the best one among the considered models and therefore this should be used to describe the environmental data upon analysis. The ML estimates of the selected model parameters and their corresponding estimated asymptotic standard errors, estimated by using the robust covariance matrix method (Bhatti 2010) and indicated in parenthesis, are:

$$\begin{aligned} \widehat{\beta}_0 &= 0.382\,(0.0030), \quad \widehat{\beta}_1 = 0.1884\,(0.0093), \\ \widehat{\varphi} &= 0.0045\,(0.0021), \quad \widehat{\alpha} = 0.2323\,(0.0460), \end{aligned}$$

and $\widehat{\alpha} = 0.2323\,(0.0460)$. These standard errors are small indicating all the parameters are estimated with good statistical precision and allow us to infer they must be part of the model. Therefore, the estimated model is $\widehat{Q}_i = (0.3821 + 0.1884\,x_{i1})^2$, for $i = 1, \ldots, 82$, while the scale-dependence matrix is estimated as $\widehat{\boldsymbol{\Gamma}} = \boldsymbol{\Gamma}(\widehat{\varphi})$, with $\boldsymbol{\Gamma}(\varphi)$ being defined in (8) for $\delta = 0.5$ and evaluated at $\widehat{\varphi} = 0.0045$.

6.3 Spatial dependence, residuals analysis, and model fitting

Note that the parameter φ is significant at 5% using the confidence interval-method, which means that exists spatial dependence.

The quantile versus quantile (QQ) plot of the residuals transformed by the Wilson-Hilferty approximation (Marchant et al. 2016b), after removing a location which was outside the bands, is displayed in Fig. 3a. An alternative method to evaluate the fit of the model is to employ the randomized quantile residual defined by Dunn and Smyth (1996). Observe that most of the residuals are inside of the bands (at 1%). In addition, Fig. 3b shows a three-

Table 2 Descriptive statistics for Mg data (in cmolc/dm3)

Median	Mean	SD	Coef. variation	Coef. skewness	Coef. kurtosis	Minimum	Maximum	n
2.0306	2.008	0.7713	0.3841	0.3394	2.9717	0.5734	4.25380	82

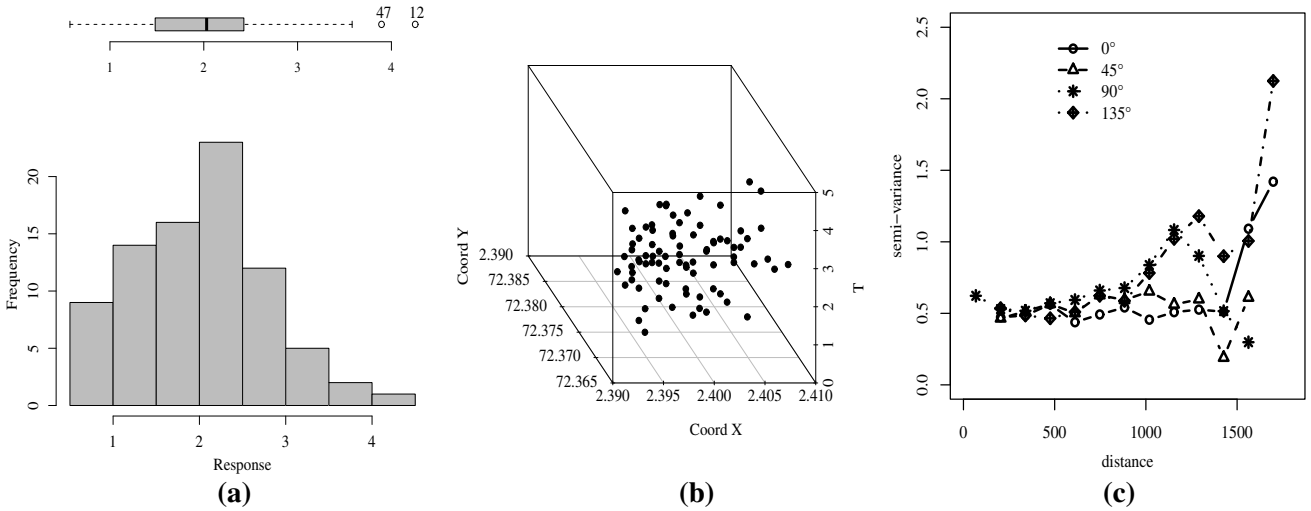

Fig. 2 (**a**) Histogram with boxplot, (**b**) scatterplot, and (**c**) semi-variogram for the response variable of environmental data

Table 3 Values of log-likelihood, CAIC and BIC for indicated models with environmental data

Model	$\ell(\widehat{\boldsymbol{\theta}})$	CAIC	BIC
Gaussian	− 32.1411	70.5900	77.5024
BS-identity link	− 36.3659	81.2513	90.3587
BS-logarithm link	− 36.3659	81.2513	90.3587
BS-square root link	− 24.9112	58.3419	67.4493

dimensional scatter plot of the estimated and observed values for the response. These two graphical plots permit us to detect a good fit of the BS spatial quantile regression model with square root link to the data. Thus, our model seems to be appropriate to describe the environmental data. However, if we use a heavy-tailed asymmetric distribution, such as the BS-Student-t model, we could obtain a better fitting, which implies further research this in line.

6.4 Global and local influence diagnostic analytics

Figure 4 presents the potentially influential cases in the ML estimates of the parameter vector $\boldsymbol{\theta}$ considering the CD as criterion of global influence. It is possible to see that cases #5, #31, #40 and #73 are potentially influential for the estimate of $\boldsymbol{\theta}$ because their values of CD are outside of the cut-off point.

For local influence, we assume two types of scheme: (1) perturbation in the response; and (2) perturbation in the explanatory variable X. We consider three measures of local influence: (1) the absolute value of the components of $\boldsymbol{d}_{\max}$; (2) normal curvature in the direction of basis vectors (C_i); and (3) conformal curvature in the same direction (B_i). Figure 5 displays the local influence graphs corresponding to perturbations in the response and explanatory variable. Note that all cases detected in the global influence plots are not locally influential by the plots associated with $\boldsymbol{d}_{\max}$, C_i and B_i when the response or explanatory variable are perturbed. For the response, observe that three cases (#17, #28 and #81) are detected as potentially influential points in two plots. For explanatory variable perturbation, we again detect the three earlier cases as potentially influential, but also cases #50 and #54; see plots (f) and (g). Note that no outliers are detected as potentially influential in plots of diagnostics, that is, in spatial statistics, an influential point is not necessarily an outlier and viceversa.

We study the relative change (RC) when cases detected as potentially influential are removed, that is, cases #17, #28 and #81, which are the points detected for the most of the plots in Figs. 4 and 5. We consider removing individual cases and combinations of them. The impact of the potentially influential cases on the parameter estimates is evaluated by computing $\mathrm{RC}_{\theta_{j(I_k)}} = |(\widehat{\theta}_j - \widehat{\theta}_{j(I_k)})/\widehat{\theta}_j| \times 100\%$, where $\widehat{\theta}_{j(I_k)}$ is the ML estimate of θ_j after removing the subset I_k, for $j = 1, \ldots, 4$ and $k = 1, \ldots, 7$, with $\theta_1 = \beta_0$, $\theta_2 = \beta_1$, $\theta_3 = \varphi$ and $\theta_4 = \alpha$. The RCs in the parameter estimates obtained by considering the data with removed cases are presented in Table 4. In general, the RCs are larger for the parameters β_0 and β_1. Note that only when cases #17 and #81 are removed simultaneously the parameter φ is not significant, and φ and α presents the largest changes. In all other cases, each parameter is significant. When analyzing the p-values of the corresponding t-tests (see values in parentheses in Table 4), note that β_0, β_1 and φ do not change their significance, but φ changes. This indicates that the detection of potentially influential

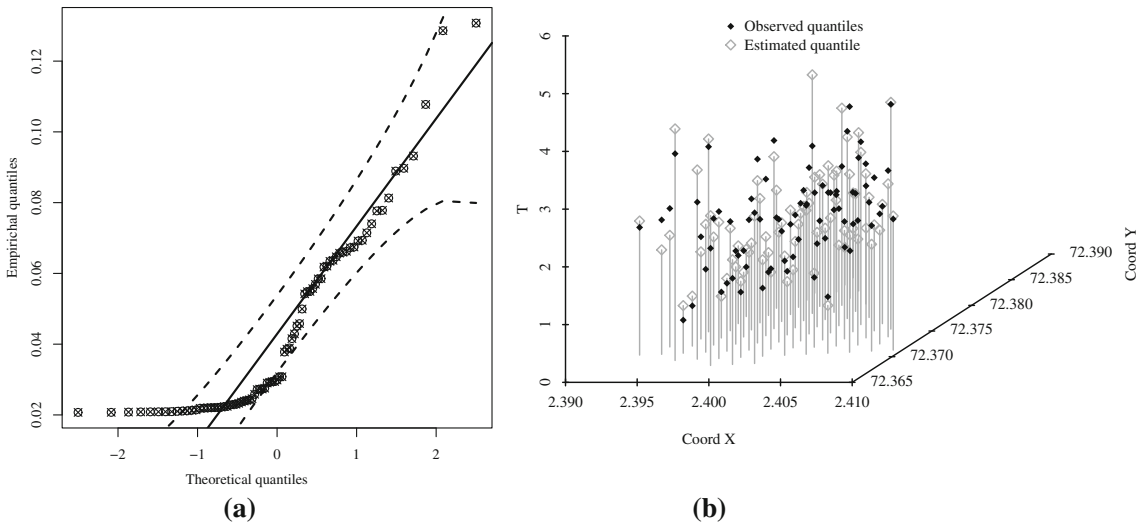

Fig. 3 **(a)** QQ plots for transformed residuals and **(b)** three-dimensional scatter plots of estimated versus observed response values with environmental data

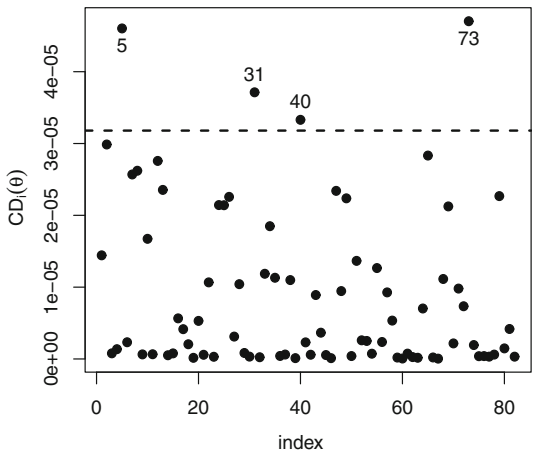

Fig. 4 Plots of the CD with environmental data

cases alters the conclusions of the study. Therefore, we conclude that removing the potentially influential cases can modify the spatial dependence and then our predictive model can be affected changing the conclusions of the study.

7 Conclusions and future works

This paper reported the following findings:

1. A geostatistical model based on a new approach to quantile regression considering the multivariate Birnbaum–Saunders distribution was formulated and the maximum likelihood estimation of their parameters was performed.
2. Global and local influence diagnostic analytics were derived for this model based on the Cook and likelihood distances, respectively.
3. An illustration of the proposed methodology was considered using an example related to environmental data to show potential applications.

In summary, we developed a novel Birnbaum–Saunders spatial quantile regression model to describing data generated from a positive skew distribution. The principal characteristic of this spatial model is the description of a quantile for a response variable that follows the Birnbaum–Saunders distribution. The numerical evaluation reported the excellent performance of the new spatial model, indicating that the Birnbaum–Saunders distribution is a good modeling choice when dealing with data which have spatial dependence, positive support and follow a distribution skewed to the right. Therefore, our investigation may be a relevant addition to the tool-kit of engineers, applied statisticians, and data scientists.

Applications of the new Birnbaum–Saunders spatial quantile regression are of interest in household income data which must be georeferenced to model them spatially. Also, georeferenced criminal, epidemiological, political, socio-economic data, where an asymmetric behavior is detected for its distribution, could be described by this new model. Some open problems that arose from the present investigation to be studied in further works are the following:

1. A test for independence can be proposed considering H_0: $\rho_{ij} = 0$ (or $\mathbf{\Gamma} = \boldsymbol{I}_n$) based on the likelihood ratio test.

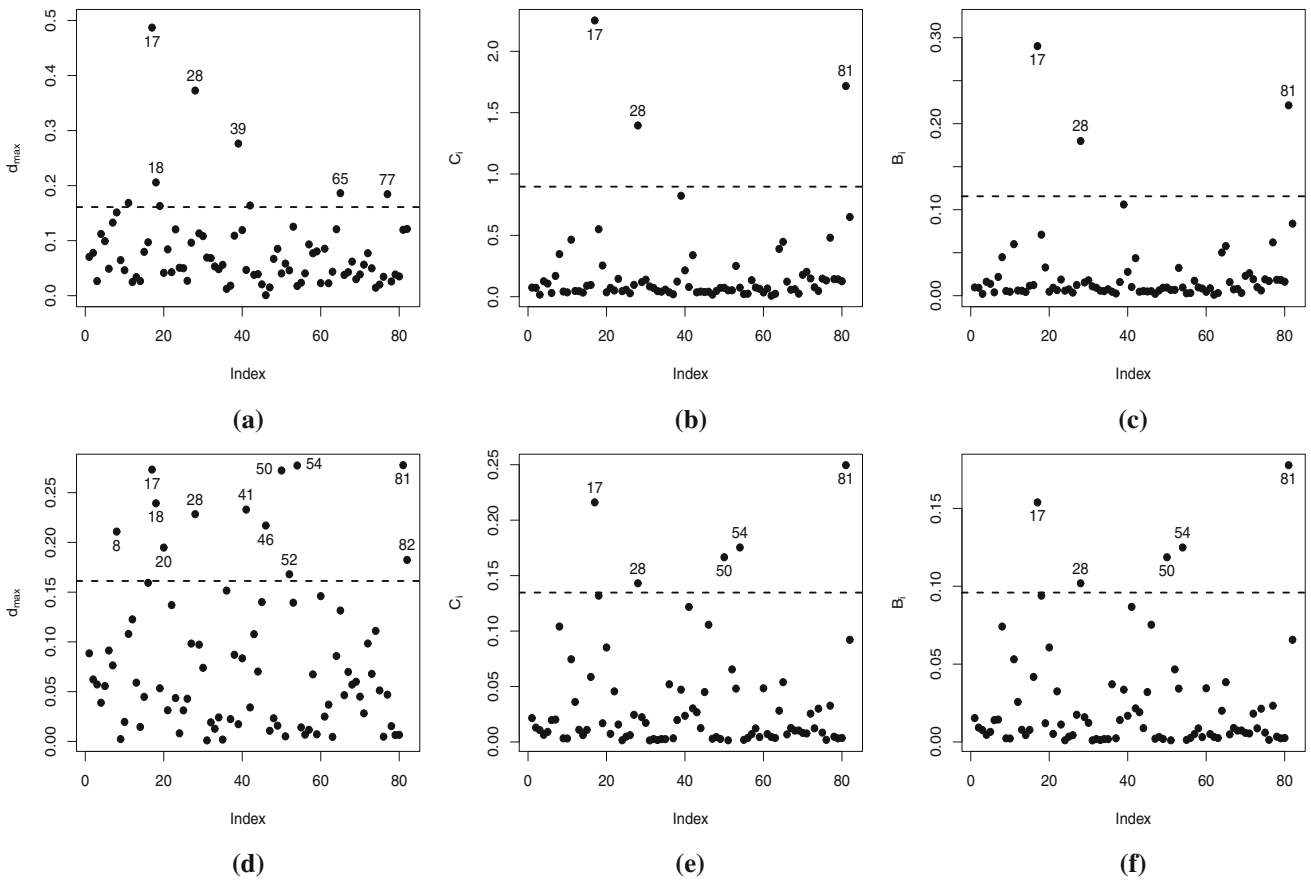

Fig. 5 Perturbation in the response for (**a**) $\boldsymbol{d}_{\max}$, (**b**) C_i and (**c**) B_i and perturbation in the regressor for (**d**) $\boldsymbol{d}_{\max}$, (**e**) C_i and (**f**) B_i with environmental data

Table 4 RC in % of ML estimates for the indicated parameter and removed cases (and p-values in parentheses) with environmental data

Removed case(s)	β_0	β_1	φ	α
None	–	–	–	–
	(2×10^{-16})	(2×10^{-16})	(0.03)	(4×10^{-7})
#17	8.0283	8.8422	3.7003	4.3282
	(2×10^{-16})	(2×10^{-16})	(4×10^{-4})	(2×10^{-16})
#28	3.9514	5.8981	8.2019	3.3356
	(2×10^{-16})	(2×10^{-16})	(5×10^{-8})	(2×10^{-16})
#81	5.0068	1.2219	1.5097	1.6262
	(2×10^{-16})	(2×10^{-16})	(2×10^{-12})	(2×10^{-16})
#17, #28	15.1840	8.6900	1.2410	4.4255
	(2×10^{-16})	(2×10^{-16})	(2×10^{-08})	(2×10^{-16})
#17, #81	1.3742	3.0580	29.5218	17.1233
	(2×10^{-16})	(2×10^{-16})	(0.2)	(4×10^{-4})
#28, #81	4.6209	1.7029	1.3709	3.1269
	(2×10^{-16})	(2×10^{-16})	(2×10^{-16})	(2×10^{-16})
#17, #28, #81	7.7262	6.0797	2.1668	6.4591
	(2×10^{-16})	(2×10^{-16})	(2×10^{-16})	(2×10^{-16})

2. The hypothesis H_0: $\varphi = 0$ versus H_1: $\varphi > 0$ can be contrasted using the likelihood ratio test.
3. The asymptotic behavior and performance of maximum likelihood estimators is also of interest, but applicability of asymptotic frameworks to spatial data is not an easy aspect; see Genton and Zhang (2012).
4. The Birnbaum–Saunders distribution is generated from the standard normal distribution and then its parameter estimation in spatial quantile regression can be affected by atypical cases. Thus, robust estimation to these cases, for example based on the Birnbaum–Saunders-t distribution, may be addressed to diminish their effects; see (Athayde et al. 2019).
5. Random effects may also be considered producing more sophisticated Birnbaum–Saunders spatial quantile regressions; see (Villegas et al. 2011).
6. Other perturbation schemes for local influence diagnostics can be conducted for Birnbaum–Saunders spatial quantile regression models.

Research on these and other issues are in progress and their findings will be reported in future articles.

Acknowledgements The authors would like to thank the Editors and Reviewers for their constructive comments which led to improve the presentation of the manuscript. The research was partially supported by the project grants "FONDECYT 1200525" from the National Commission for Scientific and Technological Research of the Chilean government (V. Leiva) and "Puente 001/2019" from the Research Directorate of the Vice President for Research of the Pontificia Universidad Católica de Chile, Chile (M. Galea).

Appendix: Perturbation matrices for the BS spatial model

For the model defined by (5) and its corresponding log-likelihood function given in (10), we have

$$\frac{\partial \ell(\boldsymbol{\theta};\boldsymbol{\omega})}{\partial \omega_i} = -\tilde{\boldsymbol{A}}_{\boldsymbol{\omega}}^{\top}\boldsymbol{\Gamma}^{-1}\frac{\partial \tilde{\boldsymbol{A}}_{\boldsymbol{\omega}}}{\partial \omega_i} + \frac{\partial}{\partial \omega_i}(\log(\tilde{a}_{\boldsymbol{\omega}})).$$

The corresponding $(p+2)\times n$ perturbation matrix is given by $\boldsymbol{\Delta} = (\partial \ell^2(\boldsymbol{\theta};\boldsymbol{\omega})/\partial\theta_j\omega_i)$, where $j = 1,\ldots,p+2$ and $i = 1,\ldots,n$, with $\theta_1 = \beta_0, \ldots \theta_p = \beta_{p-1}$, $\theta_{p+1} = \varphi$ and $\theta_{p+2} = \alpha$. The elements of this matrix are given by

$$\begin{aligned}
\frac{\partial \ell^2(\boldsymbol{\theta};\boldsymbol{\omega})}{\partial \beta_j \partial \omega_i} &= -\left(\left(\frac{\partial \tilde{\boldsymbol{A}}_{\boldsymbol{\omega}}}{\partial \beta_j}\right)^{\top}\boldsymbol{\Gamma}^{-1}\frac{\partial \tilde{\boldsymbol{A}}_{\boldsymbol{\omega}}}{\partial \omega_i} + \tilde{\boldsymbol{A}}_{\boldsymbol{\omega}}^{\top}\boldsymbol{\Gamma}^{-1}\frac{\partial^2 \tilde{\boldsymbol{A}}_{\boldsymbol{\omega}}}{\partial \omega_i \partial \beta_j}\right) + \frac{\partial}{\partial \beta_j}\left(\frac{\partial \log(\tilde{a}_{\boldsymbol{\omega}})}{\partial \omega_i}\right),\\
\frac{\partial \ell^2(\boldsymbol{\theta};\boldsymbol{\omega})}{\partial \varphi \partial \omega_i} &= -\left(\left(\frac{\partial \tilde{\boldsymbol{A}}_{\boldsymbol{\omega}}}{\partial \varphi}\right)^{\top}\boldsymbol{\Gamma}^{-1}\frac{\partial \tilde{\boldsymbol{A}}_{\boldsymbol{\omega}}}{\partial \omega_i} + \tilde{\boldsymbol{A}}_{\boldsymbol{\omega}}^{\top}\frac{\partial \boldsymbol{\Gamma}^{-1}}{\partial \varphi}\frac{\partial \tilde{\boldsymbol{A}}_{\boldsymbol{\omega}}}{\partial \omega_i}\right.\\
&\quad \left. + \tilde{\boldsymbol{A}}_{\boldsymbol{\omega}}^{\top}\boldsymbol{\Gamma}^{-1}\frac{\partial^2 \tilde{\boldsymbol{A}}_{\boldsymbol{\omega}}}{\partial \omega_i \partial \varphi}\right) + \frac{\partial}{\partial \beta_j}\left(\frac{\partial \log(\tilde{a}_{\boldsymbol{\omega}})}{\partial \omega_i}\right),\\
\frac{\partial \ell^2(\boldsymbol{\theta};\boldsymbol{\omega})}{\partial \alpha \partial \omega_i} &= -\left(\left(\frac{\partial \tilde{\boldsymbol{A}}_{\boldsymbol{\omega}}}{\partial \alpha}\right)^{\top}\boldsymbol{\Gamma}^{-1}\frac{\partial \tilde{\boldsymbol{A}}_{\boldsymbol{\omega}}}{\partial \omega_i} + \tilde{\boldsymbol{A}}_{\boldsymbol{\omega}}^{\top}\boldsymbol{\Gamma}^{-1}\frac{\partial^2 \tilde{\boldsymbol{A}}_{\boldsymbol{\omega}}}{\partial \omega_i \partial \alpha}\right) + \frac{\partial}{\partial \alpha}\left(\frac{\partial \log(\tilde{a}_{\boldsymbol{\omega}})}{\partial \omega_i}\right).
\end{aligned} \tag{23}$$

Perturbation in the response: In the case of perturbation in the response and based on its corresponding log-likelihood function given in (20), we have

$$\begin{aligned}
\frac{\partial \tilde{A}_k(\boldsymbol{\omega})}{\partial \omega_i} &= a(t_k(\boldsymbol{\omega});\alpha,Q_k)A_{ki},\\
\frac{\partial \tilde{A}_k(\boldsymbol{\omega})}{\partial \beta_j} &= -\frac{1}{\alpha\gamma_\alpha\sqrt{t_k(\boldsymbol{\omega})Q_k}}\left(\frac{t_k(\boldsymbol{\omega})\gamma_\alpha^2}{4Q_k}+1\right)\frac{1}{h'(Q_k)}x_{kj},\\
\frac{\partial^2 \tilde{A}_k(\boldsymbol{\omega})}{\partial \omega_i \partial \beta_j} &= \left(-\frac{\gamma_\alpha^2}{4Q_k}+\frac{1}{t_k(\boldsymbol{\omega})}\right)\frac{1}{2\alpha\gamma_\alpha\sqrt{Q_k t_k(\boldsymbol{\omega})}}\frac{1}{h'(Q_k)}x_{kj}A_{kj},\\
\frac{\partial}{\partial \beta_j}\left(\frac{\partial \log(\tilde{a}_{\boldsymbol{\omega}})}{\partial \omega_i}\right) &= -4\sum_{k=1}^{n}\left(\frac{t_k(\boldsymbol{\omega})\gamma_\alpha}{t_k^2(\boldsymbol{\omega})\gamma_\alpha^2+4Q_k t_k(\boldsymbol{\omega})}\right)^2\frac{1}{h'(Q_k)}x_{kj}A_{kj},\\
\frac{\partial \tilde{A}_k(\boldsymbol{\omega})}{\partial \varphi} &= a(t_k(\boldsymbol{\omega});\alpha,Q_k)\frac{\partial t_k(\boldsymbol{\omega})}{\partial \varphi},\\
\frac{\partial t_k(\boldsymbol{\omega})}{\partial \varphi} &= \left(k\text{-th row of }\frac{\partial \boldsymbol{A}}{\partial \varphi}\right)\boldsymbol{\omega},\\
\frac{\partial \boldsymbol{A}}{\partial \varphi} &= \boldsymbol{A}\left(\frac{1}{\alpha}\boldsymbol{\Gamma}^{-1/2}\frac{\partial \boldsymbol{\Gamma}^{1/2}}{\partial \varphi}\boldsymbol{\Gamma}^{-1/2}+\frac{\alpha}{4}\frac{\partial \boldsymbol{\Gamma}^{1/2}}{\partial \varphi}\right)\boldsymbol{A},\\
\frac{\partial^2 \tilde{A}_k(\boldsymbol{\omega})}{\partial \omega_i \partial \varphi} &= \frac{1}{\alpha\gamma_\alpha\sqrt{4Q_k}}\left(-\frac{1}{2t_k^{3/2}(\boldsymbol{\omega})}\left(\frac{\gamma_\alpha^2}{2}+\frac{2Q_k}{t_k(\boldsymbol{\omega})}\right)-\frac{2Q_k}{t_k^{3/2}(\boldsymbol{\omega})}\right)\\
&\quad \times\frac{\partial t_k(\boldsymbol{\omega})}{\partial \varphi}A_{ki}+a(t_k(\boldsymbol{\omega});\alpha,Q_k)\frac{\partial A_{ki}}{\partial \varphi},\\
\frac{\partial}{\partial \varphi}\left(\frac{\partial \log(\tilde{a}_{\boldsymbol{\omega}})}{\partial \omega_i}\right) &= \sum_{k=1}^{n}\left(\frac{1}{2t_k^2(\boldsymbol{\omega})}\frac{\partial t_k(\boldsymbol{\omega})}{\partial \varphi}+\frac{4Q_k}{(t_k^2(\boldsymbol{\omega})\gamma_\alpha^2+4Q_k t_k(\boldsymbol{\omega}))^2}\right.\\
&\quad \left.\times\left(2t_k(\boldsymbol{\omega})\frac{\partial t_k(\boldsymbol{\omega})}{\partial \varphi}\gamma_\alpha^2+2t_k^2(\boldsymbol{\omega})\gamma_\alpha\gamma_\alpha'+4Q_k\frac{\partial t_k(\boldsymbol{\omega})}{\partial \varphi}\right)\right)A_{ki}\\
&\quad +\sum_{k=1}^{n}\left(-\frac{1}{2t_k(\boldsymbol{\omega})}-\frac{4Q_k}{t_k^2(\boldsymbol{\omega})\gamma_\alpha^2+4Q_k t_k(\boldsymbol{\omega})}\right)\frac{\partial A_{ki}}{\partial \varphi},\\
\frac{\partial \tilde{A}_k(\boldsymbol{\omega})}{\partial \alpha} &= \frac{1}{\sqrt{4Q_k}}\left(-\frac{\gamma_\alpha+\alpha\gamma_\alpha'}{\alpha^2\gamma_\alpha^2}\left(\sqrt{t_k(\boldsymbol{\omega})}\gamma_\alpha^2-4Q_k t_k^{-1/2}(\boldsymbol{\omega})\right)\right.\\
&\quad +\frac{1}{\alpha\gamma_\alpha}\left(\frac{1}{2\sqrt{t_k(\boldsymbol{\omega})}}\frac{\partial t_k(\boldsymbol{\omega})}{\partial \alpha}\gamma_\alpha^2+2\sqrt{t_k(\boldsymbol{\omega})}\gamma_\alpha\gamma_\alpha'\right.\\
&\quad \left.\left.+2Q_k t_k^{-3/2}(\boldsymbol{\omega})\frac{\partial t_k(\boldsymbol{\omega})}{\partial \alpha}\right)\right),\\
\frac{\partial t_k(\boldsymbol{\omega})}{\partial \alpha} &= \left(k\text{-th row of }\boldsymbol{A}\left(\frac{1}{\alpha^2}\boldsymbol{\Gamma}^{-1/2}+\frac{1}{4}\boldsymbol{\Gamma}^{1/2}\right)\boldsymbol{A}\right)\boldsymbol{\omega},\\
\frac{\partial^2 \tilde{A}_k(\boldsymbol{\omega})}{\partial \omega_i \partial \alpha} &= \frac{1}{\sqrt{4Q_k}}\left(\left(-\frac{\gamma_\alpha+\alpha\gamma_\alpha'}{\alpha\gamma_\alpha}\frac{1}{\sqrt{t_k(\boldsymbol{\omega})}}-\frac{1}{2\alpha\gamma_\alpha t_k^{3/2}(\boldsymbol{\omega})}\frac{\partial t_k(\boldsymbol{\omega})}{\partial \alpha}\right)\right.\\
&\quad \times\left(\frac{\gamma_\alpha^2}{2}+\frac{2Q_k}{t_k(\boldsymbol{\omega})}\right)+\frac{1}{\alpha\gamma_\alpha}\left(\gamma_\alpha\gamma_\alpha'-\frac{2Q_k}{t_k^2(\boldsymbol{\omega})}\frac{\partial t_k(\boldsymbol{\omega})}{\partial \alpha}\right)\Big)A_{ki}\\
&\quad \left.+a(t_k(\boldsymbol{\omega});\alpha,Q_k)\left(ki\text{-th element of }\frac{\partial \boldsymbol{A}}{\partial \alpha}\right)\right),\\
\frac{\partial}{\partial \alpha}\left(\frac{\partial \log(\tilde{a}_{\boldsymbol{\omega}})}{\partial \omega_i}\right) &= \sum_{k=1}^{n}\left(\frac{1}{2t_k^2(\boldsymbol{\omega})}\frac{\partial t_k(\boldsymbol{\omega})}{\partial \alpha}+\frac{4Q_k}{(t_k^2(\boldsymbol{\omega})\gamma_\alpha^2+4Q_k t_k(\boldsymbol{\omega}))^2}\right.\\
&\quad \left.\times\left(2t_k(\boldsymbol{\omega})\frac{\partial t_k(\boldsymbol{\omega})}{\partial \alpha}\gamma_\alpha^2+2\gamma_\alpha\gamma_\alpha' t_k^2(\boldsymbol{\omega})+4Q_k\frac{\partial t_k(\boldsymbol{\omega})}{\partial \alpha}\right)\right)A_{ki}\\
&\quad +\sum_{k=1}^{n}\left(-\frac{1}{2t_k(\boldsymbol{\omega})}-\frac{4Q_k}{t_k^2(\boldsymbol{\omega})\gamma_\alpha^2+4Q_k t_k(\boldsymbol{\omega})}\right)\frac{\partial A_{ki}}{\partial \alpha},
\end{aligned}$$

where $\partial \boldsymbol{\Gamma}^{-1}/\partial\varphi = -\boldsymbol{\Gamma}^{-1}(\partial \boldsymbol{\Gamma}/\partial\varphi)\boldsymbol{\Gamma}^{-1}$, $\partial \boldsymbol{A}/\partial\alpha = \boldsymbol{A}((1/\alpha^2)\boldsymbol{\Gamma}^{-1/2} + (1/4)\boldsymbol{\Gamma}^{1/2})\boldsymbol{A}$ and A_{ki} corresponds to the ki-th element of the matrix $\boldsymbol{A}$. To calculate $\partial \boldsymbol{\Gamma}^{1/2}/\partial\varphi$, see De Bastiani et al. (2015).

Perturbation in the explanatory variable: Based on the corresponding log-likelihood function given in (22), the elements defined in (23) have as components the expressions stated as

$$\frac{\partial \tilde{A}_k(\boldsymbol{\omega})}{\partial \omega_i} = -\frac{1}{\alpha\gamma_\alpha}\left(\frac{t_k}{Q_k(\boldsymbol{\omega})}\right)^{1/2}\left(\frac{\gamma_\alpha^2}{4Q_k(\boldsymbol{\omega})}+1\right)\frac{1}{h'(Q_k(\boldsymbol{\omega}))}\beta_l A_{ki},$$

$$\frac{\partial \tilde{A}_k(\boldsymbol{\omega})}{\partial \beta_j} = -\frac{1}{\alpha\gamma_\alpha}\left(\frac{t_k}{Q_k(\boldsymbol{\omega})}\right)^{1/2}\left(\frac{\gamma_\alpha^2}{4Q_k(\boldsymbol{\omega})}+1\right)\frac{1}{h'(Q_k(\boldsymbol{\omega}))}Z_{kj},$$

$$\frac{\partial^2 \tilde{A}_k(\boldsymbol{\omega})}{\partial \omega_i \partial \beta_j} = \frac{1}{\alpha\gamma_\alpha}\left(\frac{t_k}{Q_k(\boldsymbol{\omega})}\right)^{1/2}\left(\left(\frac{3\gamma_\alpha^2}{8Q_k^2(\boldsymbol{\omega})}+\frac{1}{2Q_k(\boldsymbol{\omega})}\right) + \left(\frac{\gamma_\alpha^2}{4Q_k(\boldsymbol{\omega})}+1\right)\frac{h''(Q_k(\boldsymbol{\omega}))}{(h'(Q_k(\boldsymbol{\omega})))^2}\right)\frac{1}{h'(Q_k(\boldsymbol{\omega}))}\beta_l A_{ki} Z_{kj},$$

$$\frac{\partial}{\partial\beta_j}\left(\frac{\partial \log(\tilde{a}_\omega)}{\partial\omega_i}\right) = \sum_{k=1}^{n}\left(\left(\frac{1}{2Q_k^2(\boldsymbol{\omega})} - \frac{16}{(t_k\gamma_\alpha^2+4Q_k(\boldsymbol{\omega}))^2}\right)\times\frac{1}{h'(Q_k(\boldsymbol{\omega}))} + \left(\frac{1}{2Q_k(\boldsymbol{\omega})} - \frac{4}{t_k\gamma_\alpha^2+4Q_k(\boldsymbol{\omega})}\right)\times\frac{h''(Q_k(\boldsymbol{\omega}))}{(h'(Q_k(\boldsymbol{\omega})))^2}\right)\frac{1}{h'(Q_k(\boldsymbol{\omega}))}\beta_l A_{ki} Z_{kj} + \sum_{k=1}^{n}\left(-\frac{1}{2Q_k(\boldsymbol{\omega})} + \frac{4}{t_k\gamma_\alpha^2+4Q_k(\boldsymbol{\omega})}\right)\frac{1}{h'(Q_k(\boldsymbol{\omega}))}A_{ki}\rho_{jl},$$

$$\frac{\partial \tilde{A}_k(\boldsymbol{\omega})}{\partial \varphi} = -\frac{1}{\alpha\gamma_\alpha}\left(\frac{t_k}{Q_k(\boldsymbol{\omega})}\right)^{1/2}\left(\frac{\gamma_\alpha^2}{4Q_k(\boldsymbol{\omega})}+1\right)\frac{1}{h'(Q_k(\boldsymbol{\omega}))}\frac{\partial \boldsymbol{A}_k}{\partial\varphi}\boldsymbol{\omega},$$

$$\frac{\partial^2 \tilde{A}_k(\boldsymbol{\omega})}{\partial \omega_i \partial \varphi} = \beta_l\left(\frac{1}{\alpha\gamma_\alpha}\left(\frac{t_k}{Q_k(\boldsymbol{\omega})}\right)^{1/2}\left(\left(\frac{3\gamma_\alpha^2}{8Q_k^2(\boldsymbol{\omega})}+\frac{1}{2Q_k(\boldsymbol{\omega})}\right)\times\frac{1}{h'(Q_k(\boldsymbol{\omega}))} + + \left(\frac{\gamma_\alpha^2}{4Q_k(\boldsymbol{\omega})}+1\right)\frac{h''(Q_k(\boldsymbol{\omega}))}{(h'(Q_k(\boldsymbol{\omega})))^2}\right)\times\frac{1}{h'(Q_k(\boldsymbol{\omega}))}\frac{\partial Q_k(\boldsymbol{\omega})}{\partial\varphi}\frac{\partial \boldsymbol{A}_k}{\partial\varphi}\boldsymbol{\omega}A_{ki} - \frac{1}{\alpha\gamma_\alpha}\left(\frac{t_k}{Q_k(\boldsymbol{\omega})}\right)^{1/2}\left(\frac{\gamma_\alpha^2}{4Q_k(\boldsymbol{\omega})}+1\right)\frac{1}{h'(Q_k(\boldsymbol{\omega}))}\frac{\partial A_{ki}}{\partial\varphi}\right),$$

$$\frac{\partial}{\partial\varphi}\left(\frac{\partial \log(\tilde{a}_\omega)}{\partial\omega_i}\right) = \beta_l\sum_{k=1}^{n}\left(\left(\left(\frac{1}{2Q_k^2(\boldsymbol{\omega})} - \frac{16}{(t_k\gamma_\alpha^2+4Q_k(\boldsymbol{\omega}))^2}\right)\frac{1}{h'(Q_k(\boldsymbol{\omega}))} + \left(\frac{1}{2Q_k(\boldsymbol{\omega})} - \frac{4}{t_k\gamma_\alpha^2+4Q_k(\boldsymbol{\omega})}\right)\frac{h''(Q_k(\boldsymbol{\omega}))}{(h'(Q_k(\boldsymbol{\omega})))^2}\right)\times\frac{1}{h'(Q_k(\boldsymbol{\omega}))}\frac{\partial Q_k(\boldsymbol{\omega})}{\partial\varphi}A_{ki} + \left(-\frac{1}{2Q_k(\boldsymbol{\omega})} + \frac{4}{t_k\gamma_\alpha^2+4Q_k(\boldsymbol{\omega})}\right)\frac{1}{h'(Q_k(\boldsymbol{\omega}))}\frac{\partial A_{ki}}{\partial\varphi}\right),$$

$$\frac{\partial \tilde{A}_k(\boldsymbol{\omega})}{\partial \alpha} = \frac{1}{\sqrt{4t_k}}\left(-\frac{\gamma_\alpha+\alpha\gamma'_\alpha}{\alpha^2\gamma_\alpha^2}\left(\frac{t_k\gamma_\alpha^2-4Q_k(\boldsymbol{\omega})}{\sqrt{Q_k(\boldsymbol{\omega})}}\right) + \frac{1}{\alpha\gamma_\alpha Q_k(\boldsymbol{\omega})}\left(\left(2t_k\gamma_\alpha\gamma'_\alpha - \frac{4\partial Q_k(\boldsymbol{\omega})}{\partial\alpha}\right)\sqrt{Q_k(\boldsymbol{\omega})} - \frac{1}{2\sqrt{Q_k(\boldsymbol{\omega})}}\frac{\partial Q_k(\boldsymbol{\omega})}{\partial\alpha}(t_k\gamma_\alpha^2-4Q_k(\boldsymbol{\omega}))\right)\right),$$

$$\frac{\partial Q_k(\boldsymbol{\omega})}{\partial\alpha} = \frac{1}{h'(Q_k(\boldsymbol{\omega}))}\beta_l\frac{\partial \boldsymbol{A}_k}{\partial\alpha}\boldsymbol{\omega},$$

$$\frac{\partial^2 \tilde{A}_k(\boldsymbol{\omega})}{\partial \omega_i \partial \alpha} = -\beta_l\left(-\frac{\gamma_\alpha+\alpha\gamma'_\alpha}{\alpha^2\gamma_\alpha^2}\left(\frac{t_k}{Q_k(\boldsymbol{\omega})}\right)^{1/2}\times\left(\frac{\gamma_\alpha^2}{4Q_k(\boldsymbol{\omega})}+1\right)\frac{1}{h'(Q_k(\boldsymbol{\omega}))}A_{ki} + \frac{1}{\alpha\gamma_\alpha}\left(-\frac{1}{2}\left(\frac{Q_k(\boldsymbol{\omega})}{t_k}\right)^{-3/2}\frac{1}{t_k}\frac{\partial Q_k(\boldsymbol{\omega})}{\partial\alpha}\right)\times\left(\frac{\gamma_\alpha^2}{4Q_k(\boldsymbol{\omega})}+1\right)\frac{1}{h'(Q_k(\boldsymbol{\omega}))}A_{ki} + \frac{1}{\alpha\gamma_\alpha}\times\left(\frac{t_k}{Q_k(\boldsymbol{\omega})}\right)^{1/2}\left(\frac{8\gamma_\alpha\gamma'_\alpha Q_k(\boldsymbol{\omega}) - \frac{4\partial Q_k(\boldsymbol{\omega})}{\partial\alpha}\gamma_\alpha^2}{16Q_k^2(\boldsymbol{\omega})}\right)\frac{1}{h'(Q_k(\boldsymbol{\omega}))}A_{ki} + \frac{1}{\alpha\gamma_\alpha}\left(\frac{t_k}{Q_k(\boldsymbol{\omega})}\right)^{1/2}\left(\frac{\gamma_\alpha^2}{4Q_k(\boldsymbol{\omega})}+1\right)\times\left(-\frac{1}{(h'(Q_k(\boldsymbol{\omega})))^2}\right)h''(Q_k(\boldsymbol{\omega}))\frac{\partial Q_k(\boldsymbol{\omega})}{\partial\alpha}A_{ki} + \frac{1}{\alpha\gamma_\alpha}\left(\frac{t_k}{Q_k(\boldsymbol{\omega})}\right)^{1/2}\left(\frac{\gamma_\alpha^2}{4Q_k(\boldsymbol{\omega})}+1\right)\frac{1}{h'(Q_k(\boldsymbol{\omega}))}\frac{\partial A_{ki}}{\partial\alpha}\right),$$

$$\frac{\partial}{\partial\alpha}\left(\frac{\partial \log(\tilde{a}_\omega)}{\partial\omega_i}\right) = \beta_l\sum_{k=1}^{n}\left(\left(\frac{1}{2Q_k^2(\boldsymbol{\omega})}\frac{\partial Q_k(\boldsymbol{\omega})}{\partial\alpha} - \frac{8t_k\gamma_\alpha\gamma'_\alpha + 4\frac{\partial Q_k(\boldsymbol{\omega})}{\partial\alpha}}{(t_k\gamma_\alpha^2+4Q_k(\boldsymbol{\omega}))^2}\right)\frac{1}{h'(Q_k(\boldsymbol{\omega}))}A_{ki} + \left(-\frac{1}{2Q_k(\boldsymbol{\omega})} + \frac{4}{t_k\gamma_\alpha^2+4Q_k(\boldsymbol{\omega})}\right)\times\left(-\frac{h''(Q_k(\boldsymbol{\omega}))}{(h'(Q_k(\boldsymbol{\omega})))^2}\right)\frac{\partial Q_k(\boldsymbol{\omega})}{\partial\alpha}A_{ki} + \left(-\frac{1}{2Q_k(\boldsymbol{\omega})} + \frac{4}{t_k\gamma_\alpha^2+4Q_k(\boldsymbol{\omega})}\right)\frac{1}{h'(Q_k(\boldsymbol{\omega}))}\frac{\partial A_{ki}}{\partial\alpha}\right),$$

where $\rho_{jl} = 1$, if $j = l$; $\rho_{jl} = 0$, if $j \neq l$; $Z_{kj} = 1$ for $j = 1$; $Z_{kj} = X_{kl}(\boldsymbol{\omega})$, if $j = l$; $Z_{kj} = X_{kj}$, for $j \neq 1, l$; and $\boldsymbol{A}_k$ corresponds to the k-th row of $\boldsymbol{A}$.

References

Athayde E, Azevedo A, Barros M, Leiva V (2019) Failure rate of Birnbaum–Saunders distributions: shape, change-point, estimation and robustness. Braz J Probab Stat 33:301–328

Aykroyd RG, Leiva V, Marchant C (2018) Multivariate Birnbaum–Saunders distributions: modelling and applications. Risks 6(1), article 21

Balakrishnan N, Kundu D (2019) Birnbaum–Saunders distribution: a review of models, analysis, and application. Appl Stoch Models Bus Ind 35:4–49

Bhatti C (2010) The Birnbaum–Saunders autoregressive conditional duration model. Math Comput Simul 80:2063–2078

Birnbaum ZW, Saunders SC (1969) A new family of life distributions. J Appl Probab 6:319–327

Budsaba K, Patthanangkoor P, Volodin A (2020) A probabilistic model of growth for two-sided cracks based on the physical description of the phenomenon. Thail Stat 18:16–26

Carrasco JMF, Leiva V, Riquelme M, Aykroyd RG (2020) An errors-in-variables model based on the Birnbaum–Saunders the distribution and its diagnostics with an application to earthquake data. Stoch Environ Res Risk Assess 34:369–380

Cavieres MF, Leiva V, Marchant C, Rojas F (2020) A methodology for data-driven decision making in the monitoring of particulate matter environmental contamination in Santiago of Chile. Rev Environ Contam Toxicol. https://doi.org/10.1007/398_2020_41

Cook RD (1987) Influence assessment. J Appl Stat 14:117–131

Cook RD, Weisberg S (1982) Residuals and influence in regression. Chapman and Hall, London

Cook RD, Peña D, Weisberg S (1988) The likelihood displacement: a unifying principle for influence measures. Commun Stat Theory Methods 17:623–640

Dasilva A, Dias R, Leiva V, Marchant C, Saulo H (2020) Birnbaum-Saunders regression models: a comparative evaluation of three approaches. J Stat Comput Simul. https://doi.org/10.1080/00949655.2020.1782912

De Bastiani F, Cysneiros AHMA, Uribe-Opazo MA, Galea M (2015) Influence diagnostics in elliptical spatial linear models. TEST 24:322–340

De Bastiani F, Uribe-Opazo MA, Galea M, Cysneiros AHMA (2018) Case-deletion diagnostics for spatial linear mixed models. Spat Stat 28:284–303

Desousa MF, Saulo H, Leiva V, Scalco P (2018) On a tobit-Birnbaum–Saunders model with an application to antibody response to vaccine. J Appl Stat 45:932–955

Diaz-Garcia JA, Galea M, Leiva V (2003) Influence diagnostics for elliptical multivariate linear regression models. Commun Stat Theory Methods 32:625–641

Diggle P, Ribeiro P (2007) Model-based geoestatistics. Springer, New York

Dunn P, Smyth G (1996) Randomized quantile residuals. J Comput Graph Stat 5:236–244

Ferreira M, Gomes MI, Leiva V (2012) On an extreme value version of the Birnbaum–Saunders distribution. REVSTAT 10:181–210

Garcia-Papani F, Uribe-Opazo MA, Leiva V, Aykroyd RG (2017) Birnbaum–Saunders spatial modelling and diagnostics applied to agricultural engineering data. Stoch Environ Res Risk Assess 31:105–124

Garcia-Papani F, Leiva V, Ruggeri F, Uribe-Opazo MA (2018a) Kriging with external drift in a Birnbaum–Saunders geostatistical model. Stoch Environ Res Risk Assess 32:1517–1530

Garcia-Papani F, Leiva V, Uribe-Opazo MA, Aykroyd RG (2018b) Birnbaum–Saunders spatial regression models: diagnostics an application to chemical data. Chemom Intell Lab Syst 177:114–128

Genton MG, Zhang H (2012) Identifiability problems in some non-Gaussian spatial random fields. Chilean J Stat 3:171–179

Gradshteyn I, Ryzhik I (2000) Tables of integrals, series and products. Academic Press, New York

Huerta M, Leiva V, Rodriguez M, Liu S, Villegas D (2019) On a partial least squares regression model for asymmetric data with a chemical application in mining. Chemom Intell Lab Syst 1190:55–68

Koenker R, Bassett G (1978) Regression quantiles. Econometrica 46:33–50

Kostov P (2009) A spatial quantile regression hedonic model of agricultural land prices. Spat Econ Anal 4:53–72

Krzanowski W (1998) An introduction to statistical modelling. Arnold, London

Kundu D (2015) Bivariate sinh-normal distribution and a related model. Braz J Probab Stat 20:590–607

Lange K (2001) Numerical analysis for statisticians. Springer, New York

Leao J, Leiva V, Saulo H, Tomazella V (2018a) Incorporation of frailties into a cure rate regression model and its diagnostics and application to melanoma data. Stat Med 37:4421–4440

Leao J, Leiva V, Saulo H, Tomazella V (2018b) A survival model with Birnbaum–Saunders frailty for uncensored and censored cancer data. Braz J Probab Stat 32:707–729

Leiva V (2016) The Birnbaum–Saunders distribution. Academic Press, New York

Leiva V (2019) An interview with Sam C. Saunders. Appl Stoch Models Bus Ind 35:133–137

Leiva V, Saunders SC (2015) Cumulative damage models. In: Balakrishnan N, Colton T, Everitt B, Piegorsch W, Ruggeri F, Teugels JL (eds) Wiley StatsRef: statistics reference online. https://doi.org/10.1002/9781118445112.stat02136.pub2

Leiva V, Santos-Neto M, Cysneiros FJA, Barros M (2014) Birnbaum–Saunders statistical modeling: a new approach. Stat Model 14:21–48

Leiva V, Marchant C, Ruggeri F, Saulo H (2015) A criterion for environmental assessment using Birnbaum–Saunders attribute control charts. Environmetrics 36:463–476

Leiva V, Ferreira M, Gomes MI, Lillo C (2016a) Extreme value Birnbaum–Saunders regression models applied to environmental data. Stoch Environ Res Risk Assess 30:1045–1058

Leiva V, Santos-Neto M, Cysneiros FJA, Barros M (2016b) A methodology for stochastic inventory models based on a zero-adjusted Birnbaum–Saunders distribution. Appl Stoch Models Bus Ind 32:74–89

Leiva V, Aykroyd RG, Marchant C (2019) Discussion of "Birnbaum–Saunders distribution: a review of models, analysis, and applications" and a novel multivariate data analytics for an economics example in the textile industry. Appl Stoch Models Bus Ind 35:112–117

Lemonte A, Martínez-Florez G, Moreno-Arenas G (2015) Multivariate Birnbaum–Saunders distribution: properties and associated inference. J Stat Comput Simul 85:374–392

Lesaffre E, Verbeke G (1998) Local influence in linear mixed models. Biometrics 54:570–582

Liu Y, Mao G, Leiva V, Liu S, Tapia A (2020) Diagnostic analytics for an autoregressive model under the skew-normal distribution. Mathematics 8(5):693

Marchant C, Leiva V, Cysneiros FJA (2016a) A multivariate log-linear model for Birnbaum–Saunders distributions. IEEE Trans Reliab 65:816–827

Marchant C, Leiva V, Cysneiros FJA, Vivanco JF (2016b) Diagnostics in multivariate generalized Birnbaum–Saunders regression models. J Appl Stat 43:2829–2849

Marchant C, Leiva V, Cysneiros FJA (2018) Robust multivariate control charts based on Birnbaum–Saunders distributions. J Stat Comput Simul 88:182–202

Marchant C, Leiva V, Christakos G, Cavieres MF (2019) Monitoring urban environmental pollution by bivariate control charts: new methodology and case study in Santiago, Chile. Environmetrics 30:e2551

Martinez S, Giraldo R, Leiva V (2019) Birnbaum–Saunders functional regression models for spatial data. Stoch Environ Res Risk Assess 33:1765–1780

McMillen D (2013) Quantile regression for spatial data. Springer, New York

Nocedal J, Wright S (1999) Numerical optimization. Springer, New York

Poon WY, Poon YS (1999) Conformal normal curvature and assessment of local influence. J R Stat Soc B 61:51–61

R-Team (2018) R: a language and environment for statistical computing. R Foundation for Statistical Computing, Vienna

Sánchez L, Leiva V, Caro-Lopera FJ, Cysneiros FJA (2015) On matrix-variate Birnbaum–Saunders distributions and their estimation and application. Braz J Probab Stat 29:790–812

Sánchez L, Leiva V, Galea M, Saulo H (2020a) Birnbaum–Saunders quantile regression and its diagnostics with application to economic data. Appl Stoch Models Bus Ind. https://doi.org/10.1002/asmb.2556

Sánchez L, Leiva V, Galea M, Saulo H (2020b) Birnbaum–Saunders quantile regression models with application to spatial data. Mathematics 8(5):1000

Santana L, Vilca F, Leiva V (2011) Influence analysis in skew-Birnbaum–Saunders regression models and applications. J Appl Stat 38:1633–1649

Saulo H, Leiva V, Ziegelmann FA, Marchant C (2013) A nonparameteric method for estimating asymmetric densities based on skewed Birnbaum–Saunders distributions applied to environmental data. Stoch Environ Res Risk Asses 27:1479–1491

Saulo H, Leao J, Leiva V, Aykroyd RG (2019) Birnbaum–Saunders autoregressive conditional duration models applied to high-frequency financial data. Stat Pap 60:1605–1629

Stein ML (1999) Interpolation of spatial data: some theory for kriging. Springer, New York

Tapia A, Leiva V, Diaz MP, Giampaoli V (2019a) Influence diagnostics in mixed effects logistic regression models. TEST 28:920–942

Tapia H, Giampaoli V, Diaz MP, Leiva V (2019b) Sensitivity analysis of longitudinal count responses: a local influence approach and application to medical data. J Appl Stat 46:1021–1042

Trzpiot G (2013) Spatial quantile regression. Comp Econ Res 15:265–279

Villegas C, Paula GA, Leiva V (2011) Birnbaum–Saunders mixed models for censored reliability data analysis. IEEE Trans Reliab 60:748–758

Zhang H, Wang Y (2010) Kriging and cross-validation for massive spatial data. Environmetrics 21:290–304

Zhu H, Ibrahim JG, Lee S, Zhang H (2007) Perturbation selection and influence measures in local influence analysis. Ann Stat 35:2565–2588